



## Provenance of clastic sediments: A case study from Cameroon, Central Africa

Victorine Ambassa Bela, Armel Zacharie Eko Bessa, John S. Armstrong-Altrin, Francis Aonsi Kamani, Estelle Diane Biami Nya, Gabriel Ngueutchoua

### ► To cite this version:

Victorine Ambassa Bela, Armel Zacharie Eko Bessa, John S. Armstrong-Altrin, Francis Aonsi Kamani, Estelle Diane Biami Nya, et al.. Provenance of clastic sediments: A case study from Cameroon, Central Africa. Solid Earth Sciences, 2023, 8 (2), pp.105-122. 10.1016/j.sesci.2023.03.002 . hal-04198477

HAL Id: hal-04198477

<https://hal.science/hal-04198477>

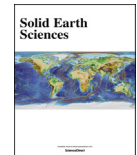
Submitted on 8 Sep 2023

**HAL** is a multi-disciplinary open access archive for the deposit and dissemination of scientific research documents, whether they are published or not. The documents may come from teaching and research institutions in France or abroad, or from public or private research centers.

L'archive ouverte pluridisciplinaire **HAL**, est destinée au dépôt et à la diffusion de documents scientifiques de niveau recherche, publiés ou non, émanant des établissements d'enseignement et de recherche français ou étrangers, des laboratoires publics ou privés.



Distributed under a Creative Commons Attribution 4.0 International License



# Provenance of clastic sediments: A case study from Cameroon, Central Africa

Victorine Ambassa Bela <sup>a</sup>, Armel Zacharie Eko Bessa <sup>a,b,\*</sup>, John S. Armstrong-Altrin <sup>c,d</sup>, Francis Aonsi Kamani <sup>a,e</sup>, Estelle Diane Biami Nya <sup>a</sup>, Gabriel Ngueutchoua <sup>a</sup>

<sup>a</sup> Department of Earth Sciences, Faculty of Science, University of Yaoundé I, Cameroon

<sup>b</sup> Department of Earth Sciences and Environment, Higher Teacher Training College, University of Bertoua, P.O. Box 652, Bertoua, Cameroon

<sup>c</sup> Universidad Nacional Autónoma de México, Instituto de Ciencias del mar y Limnología, Unidad de Procesos Oceánicos y Costeros, Circuito exterior s/n, 04510 Mexico City, Mexico

<sup>d</sup> Department of Marine Sciences, Bharathidasan University, Tiruchirapalli, 620024, Tamil Nadu, India

<sup>e</sup> Geosciences Rennes, University of Rennes 1, UMR CNRS 6118, 35000, Rennes, France

Received 13 September 2022; revised 6 March 2023; accepted 23 March 2023

Available online 10 April 2023

## Abstract

The provenance of clastic sediments in stream beds, river terraces, rivers, swamps, lakes and beaches from different geological settings was investigated based on their compositional and geochemical variations. The geochemistry data of 622 sediment samples from 22 sites in the Cameroon were compiled to infer the provenance. The results suggest that, their mineralogy is dominated by quartz, low amount of feldspars, clay minerals, heavy minerals, ferric minerals, and rock fragments. The  $\text{SiO}_2/\text{Al}_2\text{O}_3$  ratio indicate that the sediments of Cameroonian region are mostly rich in quartz and clay-minerals. The enrichment of  $\text{K}_2\text{O}/\text{Na}_2\text{O}$  ratio implies plagioclase disintegration as K-feldspar during weathering and/or K-reintroduction in the system during diagenesis. The sediments are rich in light rare earth elements (LREE) and classified as shale, Fe-shale, Fe-sand, wacke, arkose, litharenite, sublitharenite, and quartzarenite. The sediments are composed of detritus derived from felsic igneous rocks, which correspond to the geology of the source areas. Weathering indices such as chemical index of alteration (CIA), chemical index of weathering (CIW), plagioclase index of alteration (PIA) and, A-CN-K ( $A=\text{Al}_2\text{O}_3$ ,  $CN=\text{CaO}^* + \text{Na}_2\text{O}$ ,  $K=\text{K}_2\text{O}$ ) plot indicated that the source rocks are subjected to low, moderate and intense weathering.

Copyright © 2023, Guangzhou Institute of Geochemistry. Production and hosting by Elsevier B.V. This is an open access article under the CC BY license (<http://creativecommons.org/licenses/by/4.0/>).

**Keywords:** Provenance; Sediments; Weathering; Source rocks; Chemical indices; Central Africa

## 1. Introduction

Sediments are composed of fine (silt and clay) to coarse (sands) particles, are weathered and transported, in particular, by climatic changes (wind, tides, water and ice) and human

activities (development work, land use, etc.). In addition, sediments are defined as continental or marine deposits consisting of particles that come from the weathering or disintegration of pre-existing rocks and precipitation of suspended matter passing through the water column (El Houssainy, 2020; Cojan and Renard, 2021). The particles that make up the sediments are more or less large and consist of organic and inorganic compounds from four distinct sources: terrigenous, endogenous, neof ormation and anthropic (Schneider, 2001; Chapalain, 2019; Karam, 2019). Analyzing the chemical composition of terrigenous sediments is a sensitive technique for determining weathering, depositional environment, and

\* Corresponding author.

E-mail addresses: [victorineambassa1@gmail.com](mailto:victorineambassa1@gmail.com) (V. Ambassa Bela), [armeleteko@yahoo.fr](mailto:armeleteko@yahoo.fr) (A.Z. Eko Bessa), [armstrong@cmarl.unam.mx](mailto:armstrong@cmarl.unam.mx) (J.S. Armstrong-Altrin), [aonsifrancis1@gmail.com](mailto:aonsifrancis1@gmail.com) (F. Aonsi Kamani), [biaminyaestelleiane1@gmail.com](mailto:biaminyaestelleiane1@gmail.com) (E.D. Biami Nya), [ngueutschoua2@yahoo.fr](mailto:ngueutschoua2@yahoo.fr) (G. Ngueutschoua).

Peer review under responsibility of Guangzhou Institute of Geochemistry.

provenance. The type of the source rocks, climate, and tectonic aspects of the source area influence sediment composition (e.g., Armstrong-Altrin and Machain Castillo, 2016; Yu et al., 2016; Jian et al., 2020; Garzanti et al., 2021). The provenance of detrital sediments is sometimes difficult to determine due to weathering, diagenesis and climate variables, and these generate observable variations in their patterns (Lee, 2009; Armstrong-Altrin et al., 2014, 2019; Garzanti et al., 2019, 2020). Because, diagenesis and even metamorphism do not affect Th, Sc, Co, and Cr, and these elements are the most reliable elements to infer sediment provenance (Cullers, 1994). However, studies on the provenance of sediments are great interest in sedimentology, because they provide information firstly on their origin and secondly on the conditions of transport and deposition (e.g., Armstrong-Altrin et al., 2021a; Garzanti et al., 2020, 2021; Jian et al., 2020; Eko Bessa et al., 2021a). The geochemistry of clastic sediments is an essential source of information for determining their provenance history (Cullers, 2000; Ramos-Vázquez and Armstrong-Altrin, 2019, 2020; Banerji et al., 2022), as well as the degree of weathering (Roy et al., 2008; Gallala et al., 2009). Kirkwood et al. (2016), found that the chemistry of surface sediments is extremely susceptible to compositional changes. As a result, sediments are thought to provide a more complete understanding of the source domain (Silva et al., 2016; Armstrong-Altrin, 2020).

In Cameroon, sediments are fluvio-maritime in nature, they constitute the sediment load of watercourses and are lacustrine (e.g., Eko Bessa et al., 2018, 2021a, b; N'nanga et al., 2019), fluvial (e.g. Ndjigui et al., 2015, 2018; Eko Bessa et al., 2020; Nanga Bineli et al., 2020), alluvial (e.g., Mbale Ngama et al., 2019; Chougong Tchatchouang et al., 2021), clastic (e.g., Ngueutchoua et al., 2017, 2019a, b; Bokanda et al., 2019; Tchouatcha et al., 2020) and coastal (Kwewouo Janpou et al., 2022; Ambassa Bela et al., 2022). This article reviews the various potential sources of surface clastic sediments in Cameroon, considered as a reservoir of several economically important components (heavy minerals, trace and rare earth elements). In this study, we compiled the mineralogy and geochemistry data of clastic sediments from different locations in Cameroon. The purpose of this study is to determine the origin of clastic sediments in Cameroon and to provide an insight into the sediment provenance study. This study will allow to understand the geology of the area and highlight the sedimentary processes during transport and deposition.

## 2. Data sources and analytical methods

### 2.1. Literature survey and compilation of database

This study constitutes a compilation of geochemical, mineralogical, and sedimentological data of sediments (surface and clastic) in Cameroon. To collect information on the origin of sediments, including their characteristics and evolution, a literature study was conducted using google Scholar, Science

Direct and PubMed sears browsers. Based on the following inclusion criteria, at least 2000 publications were chosen for title and abstract screening: articles including the terms specified above; non-Cameroonian items and articles out of context. Certain studies were excluded, if the same paper was published in several journals; the paper had the same results but with a different title; the papers that dealt with provenance but not in Cameroon and the papers with limited data. Additional research was found by searching reference lists (Fig. 1). Twenty-two sites were identified among which 476 sediment samples (sand, clays, shale, clastic rocks, sediment deposits), were compiled.

### 2.2. Sampling description

This study compiled a huge database on the geochemistry, mineralogy, and sedimentology of surface and clastic sediments from areas with variety of tectonic settings around Cameroon, which are briefly described below: (i) sedimentary formations: Douala sub-basin (Ngueutchoua et al., 2017, 2019a, 2019b; Mbabi Bitchong et al., 2021), Mamfe basin (Ngueutchoua et al., 2019b; Bokanda et al., 2019, 2021), Babouri-Figuil and Mayo Oulo-Lere (Tchouatcha et al., 2021); (ii) river terrace: Mefou River (Mbale Ngama et al., 2019; Noa Tang et al., 2020); (iii) rivers: Lokoundje River (Ndjigui et al., 2018), Ngaye River (Ndjigui et al., 2019), Sanaga River (Nanga Bineli et al., 2020), Lobe River (Chougong Tchatchouang et al., 2021), Nyong River (Kontchipe et al., 2021), and Dibamba River (Sonfack et al., 2021); (iv) swamp: Moloundou swamp (Eko Bessa et al., 2020); (v) lakes: Simbock lake (Eko Bessa et al., 2018), Ossa Lakes Complex (Eko Bessa et al., 2021a), Ngaoundaba Lake (Eko Bessa et al., 2021b), and Fonjak Lake (N'Nanga et al., 2019); and (vi) coastal zones: Mouanko beach (Ambassa Bela et al., 2022), and Limbe beach (Kwewouo Janpou et al., 2022). These authors have described the methods of sample collection and analysis employed in their respective articles, so a description on sample types and analytical methods are not provided in this study. In short, the geographical presentation of each site will be given in Table 1 and Fig. 2.

From these studies, Chemical Index of Alteration ( $CIA = [Al_2O_3/(Al_2O_3 + CaO^* + Na_2O + K_2O)] \times 100$ ), suggested by Nesbitt and Young (1982), Chemical Index of Weathering ( $CIW = [Al_2O_3/(Al_2O_3 + CaO^* + Na_2O)] \times 100$ ) (Harnois, 1988), and Plagioclase Index of Alteration ( $PIA = [Al_2O_3 - K_2O]/(Al_2O_3 + CaO^* + Na_2O - K_2O)] \times 100$ ), proposed by Fedo et al. (1995), are used to assess weathering in the source location. The best and most often used Index, according to Armstrong-Altrin et al. (2015) and others is the CIA, which is derived from the equation presented above, where  $CaO^*$  is the quantity of  $CaO$  in the silicate component of rock. For the CIA, PIA, and CIW values, a value of 60 indicates low weathering, a value of 60–80 suggests moderate weathering, and a value of >80 indicates strong weathering intensity, with complete conversion of feldspars to aluminous clay minerals (Fedo et al., 1995).

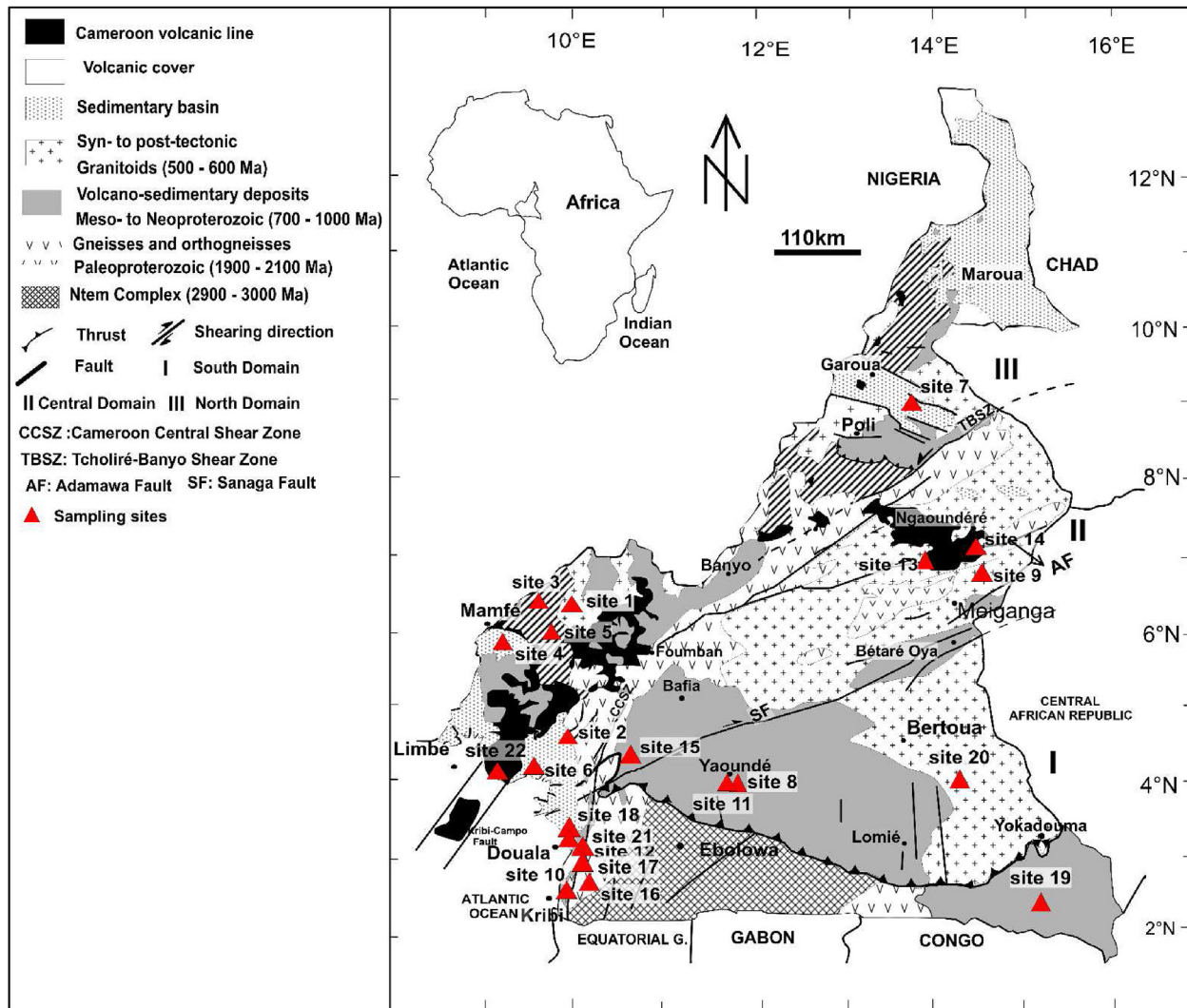


Fig. 1. Map of Cameroon showing the locations of sediments compiled at various sites.

### 3. Geological context

Cameroon is located in the Central African Region. It encompasses 475,442 km<sup>2</sup> and is located between latitudes 2° and 13°N and longitudes 9° and 16°E. Cameroon is oriented west to east from the Atlantic Ocean to the Congo, and south to north from Gabon to Lake Chad.

The Central African Region has been divided into different climatic zones, which can be divided into two major classes: tropical climate with two seasons and equatorial climate with four seasons (Donfack, 2011).

The vegetation differs between the equatorial and tropical zones, which is diverse. The equatorial zone's vegetation is primarily forest, which occupies about 45% of the country and grows increasingly dense from the coast to the east, with gallery forests along the rivers in the North. The tropical zone is mostly covered by variety of savannah types: The Adamawa woody savannah is densely forested, while the grassland savannah of the North and the steppe of the Far North are sparsely forested (Letouzey, 1985; Biwolé et al., 2015).

The variety of parent rocks, geographical characteristics, age, and varied bioclimatic conditions all contribute to the diversity of Cameroonian soils. Several soils are related to their spatial representativeness, degradation status, and human use. The principal soils of Cameroon are: (i) ferralsols or ferrallitic soils, which cover the great part of the South Cameroon plateau and those which cover the rest of the country (Nakao et al., 2017; Doum et al., 2020; Temga et al., 2021; Sababa et al., 2022). (ii) hydromorphic soils or gleysols, which are grey, discolored horizons encountered in the Lake Chad plain during the rainy season (Doum et al., 2020); (iii) poorly evolved soils formed on recent deposits, such as wind-blown deposits in the Lake Chad cordillera or volcanic ashes in West Cameroon. Vertisols have a consistent, clayey, dark-colored profile that cracks deeply in dry conditions (Tsouzue and Ndjigui, 2017; Temga et al., 2019; Eko Bessa et al., 2022). Young andosols and eutrophic brown soils have a uniform profile. They are formed on basalts and are connected with crude and poorly evolved minerals. They are rich in water and organic materials, but are extremely vulnerable to erosion. Besides that, eutrophic

Table 1

Geographic coordinates, Region/locality of the different sites of Cameroon.

Sites	Geographic coordinates		Location
	Latitudes (N)	Longitudes (E)	
1 (n = 15)	03°20'–05°00'	09°00'–10°30'	South West (DSB, Kumba)
2 (n = 21)	03°20'–05°00'	09°00'–10°00'	South West (DSB)
3 (n = 23)	05°30'–06°00'; 3°20'–05°00'	09°00'–09°30'; 9°00–09°30'	South West (Mamfe Basin; DSB)
4 (n = 24)	05°30'–06°00'	09°00'–09°00'	South West (Mamfe Basin)
5 (n = 25)	05°30'–06°00'	09°00'–09°30'	South West (Mamfe Basin)
6 (n = 64)	04°10'–04°12'	09°50'–09°52'	Littoral (DSB)
7 (n = 12)	09°42'–09°48'	13°42'–14°00'	North (Babouri-Figuil; Mayo Oulo-Lere)
8 (n = 9)	03°45'–03°58'	11°20'–11°33'	Center, Yaounde (Mefou River)
9 (n = 17)	07°10'–07°13'	14°57'–15°00'	Adamawa (Ngaye River)
10 (n = 18)	02°51'–03°12'	09°54'–10°10'	South, Kribi (Lokoundje River)
11 (n = 19)	03°45'–03°58'	11°20'–11°33'	Center, Yaounde (Simbock Lake)
12 (n = 14)	03°45'–03°53'	09°58'–10°04'	Littoral, Dizangue (Ossa Lake)
13 (n = 20)	07°07'–07°08'	13°41'–13°42'	Adamawa (Ngaoundaba Lake)
14 (n = 23)	07°09'–07°13'	13°46'–13°52'	Adamawa (Fonjak Lake)
15 (n = 17)	03°30'–04°30'	10°00'–12°00'	Center and Littoral (Sanaga River)
16 (n = 19)	02°04'–02°10'	09°09'–09°50'	South (Lobe River)
17 (n = 20)	02°48'–04°32'	09°54'–13°30'	Center (Nyong River)
18 (n = 20)	03°90'–04°40'	09°40'–10°30'	Littoral (Dibamba River)
19 (n = 30)	02°05'–02°12'	15°24'–15°42'	East (Moloundou Swamp)
20 (n = 13)	04°21'–04°51'	14°10'–14°30'	East (Kadey plain)
21 (n = 24)	03°37'–03°41'	09°37'–09°40'	Littoral (Mouanko beaches)
22 (n = 29)	03°59'–04°04'	09°01'–09°13'	South West (Limbe beaches)

DSB, Douala Sub-basin; n, number of samples.

brown soils have a lot of humus and mineral stuff. These soils are developed un top of a substratum, which is made up of different types of rocks with different ages.

The Precambrian crypts of Cameroon consist of two major structural rock units: North Pan-African Equatorial Range ([Ngnotué et al., 2000](#)) the Yaounde extreme group represents two-thirds of Cameroon North and the Cratonic domains that are bounded by the northern margin of the Congo Craton Northern Yaounde group. The CPNE is an E–W trending megachain, surrounded by the Trans-Saharan Pan-African chain to the south. It stretches from northern Brazil to the west through the “Sergipano range”, forming the Pan-African-Brazilian Range ([Brito de Neves et al., 2001](#)). [Toteu et al. \(2004\)](#) distinguish CPNE as three different geo-dynamic domains: northern, central and southern.

The North Cameroon domain is a vast domain that extends from the south to the north of Poli. This area is characterized by the development of polyphasic and polycyclic premature stages ([Nzenti et al., 1992](#)). It consists of metavolcanites related to the metasedimentary series of Poli. Calcareous metabasites and orthogneisses belonging to episodic epistasis ([Bouyo et al., 2016](#); [Nomo et al., 2017](#)). The central Cameroon domain is the northern and south of the Pan-African range of Cameroon. It is a vast area that stretches between the Sanaga faults (south of Bafia) and the Tibati-Banyo line (north of the Adamawa plateau). It contains numerous syntectonic hyperpotassic plutons with calc-alkaline affinity of Pan-African age ([Nzolang et al., 2003](#); [Nzenti et al., 2011](#)). The southern domain is mainly represented by the Yaounde Group, and the southern part is bounded by the Congo Craton. At the regional scale, two

major rock units are defined: the slightly altered shale-quartzite unit (Ayos-Mbalmayo-Bengbis and Yokaduma ridges) and an advanced unit. Metamorphism consists of gneiss, gneiss-mica, amphibole and rocks contain silicate lime (Yaounde, Ntui-Betamba and Bafia series). These two large rock units were overlain by diorite and granite and underwent high-pressure, high-temperature metamorphism ([Penaye et al., 1993](#); [Owona et al., 2011](#)). [Ngnotué et al. \(2012\)](#) indicate the presence of a new metamorphic event during the Stenian (911–1122 Ma) in the Tonian, interpreted as the onset of metamorphism in the Yaounde series.

The Congo Craton stretches from Cameroon (the northern border) to the Democratic Republic of the Congo, Congo and Angola (South) through Congo, Gabon and Equatorial Guinea (the central part) is created while the Trans-Amazonian Orogeny between 2200 and 1900 Ma (Barboza and Sabate, 2002; [Shang et al., 2007](#)). The northwestern margin of the Congo Craton is a vast area. It is located in southern Cameroon and consists of Archean and Paleoproterozoic formations. This part of Craton is known because it is made up of three Ntem complexes: the Ntem unit, the Lower Nyong unit and the Ayna unit. The Ntem unit has been affected by two orogenic cycles and is composed of various materials. The first orogenic cycle or Liberian cycle is marked by the establishment of greenstone protoliths followed by TTG (Tonalite-Trondhjemite-Granodiorite) intrusion between 2900 and 2800 Ma. Anatetic and potassic granitoids begin to appear, signaling the end of this cycle at 2600 and 2500 Ma ([Toteu et al., 2004](#); [Shang et al., 2010](#)). The second cycle is Eburnean and is characterized by three successive events: the intrusion of alkaline syenite around 2300 Ma, the placement of dolerites around 2100 Ma and

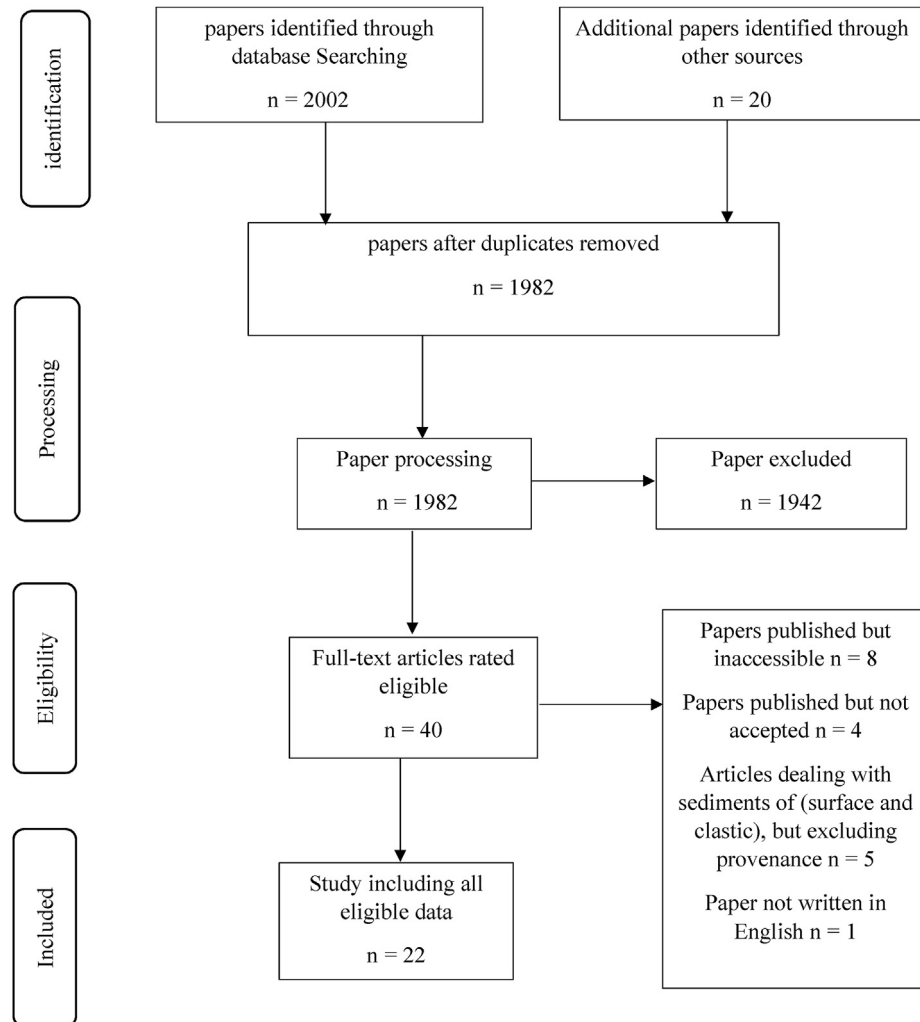


Fig. 2. Flow diagram illustrating data compilation.

finally a metamorphism of amphibolite to granulite facies around 2500 Ma.

The Lower Nyong unit is north of Ntem unit. The meta-sedimentary and metaplutonic rocks emplaced during high-grade tectonic metamorphic events around 2050 Ma. This unit is placed on the axis of the Congo Craton as an Eburnean aquifer (Feybesse et al., 1987; Tsameni and Nsifa, 1998). The rocks of the Lower Nyong unit are entirely Paleozoic and most of the protoliths are of Archean age (Lerouge et al., 2006). The Ayna unit is located at the eastern end of the Ntem complex and consists of fine-grained crystalline rocks (leptinites, granulites, amphibole, gneiss), intrusive granites (granite, syenite, tonalite) and green colored rocks (Gazel and Guiraudie, 1965).

In the coastal region (Douala and Mamfe basins), the south (Mintom basin), the north (Benoue basin), and Southern Chad sedimentary basins produce tiny subsidence zones. The coastal sedimentary basin on the edge of the Gulf of Guinea corresponds to a subsiding trench built from the Cretaceous and gradually deepening towards the Atlantic Ocean (where extensive research was conducted) (Ngon et al., 2016). Its principal formations are black marls, clays, and sandstones; in

the Douala basin in the south-west, lava flows interbred (Ngueutchoua et al., 2019a, 2019b). The Douala basin's Phanerozoic strata top Neoproterozoic gneisses and granitoids (Ngon et al., 2016), which are Sanaga River basin basement formations. Low-grade metamorphic rocks (phyllites, shales, and siliceous facies represented by quartzites generally interbedded in shales) of the Lom series near the northeastern end of the Sanaga River basin and medium to high-grade gneissic rocks of the Yaoundé Group are examples of Pan African metamorphic rocks (Owona et al., 2021). Under the "Intermediate Series" and the "Dja Formation," the Cameroon geological formations are largely Precambrian (Basement Complex), originating from the remobilization of the Archean basement (Shang et al., 2004; Asaah et al., 2014; Owona et al., 2021; Tchakounté et al., 2021). The "Ntem Complex" of Archean to Palaeoproterozoic age, which encompasses southern Cameroon and is primarily made of TTG (tonalite, trondhjemite, granitoid), and green rocks, are the Cameroonian section of the Congo Craton (Tchameni et al., 2000). The rest of the country is covered by three primary geological domains formation (North, Central, and South). The Poli and Lom

Table 2  
Mineralogical composition of sediments from the sites compiled.

	site1	site2	site3	site4	site5	site6	site7	site8	site9	site10	site11	site12	site13	site14	site15	site16	site17	site18	site19	site20	site21	site22
Quartz	n.a.	+++	+++	+++	n.a.	n.a.	n.a.	+++	+++	+++	+++	+++	+++	+++	+++	+++	+++	+++	+++	+++	+++	
Kaolinite	n.a.	+++	+++	+	n.a.	n.a.	n.a.	+	+	+	+	+	+	+	+	+	+	+	+	+	+	
Muscovite	n.a.	+	+	+	n.a.	n.a.	n.a.	n.a.	n.a.	n.a.	n.a.	n.a.	n.a.	n.a.	n.a.	n.a.	n.a.	n.a.	n.a.	n.a.	n.a.	
Illite	n.a.	-	+	+	n.a.	n.a.	n.a.	n.a.	n.a.	n.a.	n.a.	n.a.	n.a.	n.a.	n.a.	n.a.	n.a.	n.a.	n.a.	n.a.	n.a.	
Feldspar	n.a.	+	+	+	n.a.	n.a.	n.a.	n.a.	n.a.	n.a.	n.a.	n.a.	n.a.	n.a.	n.a.	n.a.	n.a.	n.a.	n.a.	n.a.	n.a.	
Hematite	n.a.	+	+	+	n.a.	n.a.	n.a.	n.a.	n.a.	n.a.	n.a.	n.a.	n.a.	n.a.	n.a.	n.a.	n.a.	n.a.	n.a.	n.a.	n.a.	
Goethite	n.a.	-	+	+	n.a.	n.a.	n.a.	n.a.	n.a.	n.a.	n.a.	n.a.	n.a.	n.a.	n.a.	n.a.	n.a.	n.a.	n.a.	n.a.	n.a.	
Rutile	n.a.	-	+	+	n.a.	n.a.	n.a.	n.a.	n.a.	n.a.	n.a.	n.a.	n.a.	n.a.	n.a.	n.a.	n.a.	n.a.	n.a.	n.a.	n.a.	
Smectites	n.a.	-	-	-	n.a.	n.a.	n.a.	n.a.	n.a.	n.a.	n.a.	n.a.	n.a.	n.a.	n.a.	n.a.	n.a.	n.a.	n.a.	n.a.	n.a.	
Amphibole	n.a.	-	-	-	n.a.	n.a.	n.a.	n.a.	n.a.	n.a.	n.a.	n.a.	n.a.	n.a.	n.a.	n.a.	n.a.	n.a.	n.a.	n.a.	n.a.	
Plagioclases	n.a.	-	-	-	n.a.	n.a.	n.a.	n.a.	n.a.	n.a.	n.a.	n.a.	n.a.	n.a.	n.a.	n.a.	n.a.	n.a.	n.a.	n.a.	n.a.	
Gibbsite	n.a.	-	-	-	n.a.	n.a.	n.a.	n.a.	n.a.	n.a.	n.a.	n.a.	n.a.	n.a.	n.a.	n.a.	n.a.	n.a.	n.a.	n.a.	n.a.	
Calcite	n.a.	-	-	-	n.a.	n.a.	n.a.	n.a.	n.a.	n.a.	n.a.	n.a.	n.a.	n.a.	n.a.	n.a.	n.a.	n.a.	n.a.	n.a.	n.a.	
Serpentine	n.a.	-	-	-	n.a.	n.a.	n.a.	n.a.	n.a.	n.a.	n.a.	n.a.	n.a.	n.a.	n.a.	n.a.	n.a.	n.a.	n.a.	n.a.	n.a.	
Anatase	n.a.	-	-	-	n.a.	n.a.	n.a.	n.a.	n.a.	n.a.	n.a.	n.a.	n.a.	n.a.	n.a.	n.a.	n.a.	n.a.	n.a.	n.a.	n.a.	
Magnetite	n.a.	-	-	-	n.a.	n.a.	n.a.	n.a.	n.a.	n.a.	n.a.	n.a.	n.a.	n.a.	n.a.	n.a.	n.a.	n.a.	n.a.	n.a.	n.a.	
Halloysite	n.a.	-	-	-	n.a.	n.a.	n.a.	n.a.	n.a.	n.a.	n.a.	n.a.	n.a.	n.a.	n.a.	n.a.	n.a.	n.a.	n.a.	n.a.	n.a.	
Chlorite	n.a.	-	-	-	n.a.	n.a.	n.a.	n.a.	n.a.	n.a.	n.a.	n.a.	n.a.	n.a.	n.a.	n.a.	n.a.	n.a.	n.a.	n.a.	n.a.	
Biotite	n.a.	-	-	-	n.a.	n.a.	n.a.	n.a.	n.a.	n.a.	n.a.	n.a.	n.a.	n.a.	n.a.	n.a.	n.a.	n.a.	n.a.	n.a.	n.a.	
Ilmenite	n.a.	-	-	-	n.a.	n.a.	n.a.	n.a.	n.a.	n.a.	n.a.	n.a.	n.a.	n.a.	n.a.	n.a.	n.a.	n.a.	n.a.	n.a.	n.a.	
Augite	n.a.	-	-	-	n.a.	n.a.	n.a.	n.a.	n.a.	n.a.	n.a.	n.a.	n.a.	n.a.	n.a.	n.a.	n.a.	n.a.	n.a.	n.a.	n.a.	

+++ (>50%) Very abundant; ++ (25–50%) Abundant; + (10–20%) Poorly represented; ε (<10%) Trace; - Not identified; n.a. Not analyzed.

groups have undergone little metamorphism. The end of the Pan-African orogeny is marked by the volcano-sedimentary deposits of Mangbei. They are part of a regional assemblage that includes outcrops in Mangbei and Hoye near Poli in the Lake Lere region (Bouyo et al., 2009, 2016; Nomo et al., 2017). In the coastal region (Douala and Mamfe basins), the south (Mintom basin), the north (Benoue basin), and Southern Chad sedimentary basins produce tiny subsidence zones. The coastal sedimentary basin on the edge of the Gulf of Guinea corresponds to a subsiding trench built from the Cretaceous and gradually deepening towards the Atlantic Ocean (Ngon et al., 2016). Its principal formations are black marls, clays, and sandstones; in the Douala basin in the south-west, lava flows interbred (Ngueutchoua et al., 2019a, 2019b). The Douala basin's Phanerozoic strata top Neoproterozoic gneisses and granitoids (Ngon et al., 2016) are the Sanaga River basin basement formations. Low-grade metamorphic rocks (phyllites, shales, and siliceous facies represented by quartzites, generally interbedded in shales) of the Lom series near the northeastern end of the Sanaga River basin and medium to high-grade gneissic rocks of the Yaoundé Group are examples of Pan-African metamorphic rocks (Owona et al., 2021).

## 4. Results

### 4.1. Mineralogy

Seventeen articles among 22 have performed X-ray diffraction analysis (Table 2), which reveals that quartz is very abundant in all these sites, but less abundant in the site of Adamawa Region. The abundance of quartz in sediments can be explained by the weathering processes of silica rich rocks. Kaolinite is abundant in almost all environments except in some rivers (Nyong, Lobe, Dibamba and Mefou). In the Mamfe basin and the Moloundou swamp they are little represented. It is very abundant in DSB. The kaolinite originated from the partial hydrolysis with severe leaching and partial depletion of silica. Minerals such as feldspars, illite, hematite, goethite, rutile, gibbsite are poorly represented in most sites (Table 2), the other minerals are either in trace, unidentified or poorly represented in the stations. Illite might have derived by the alteration of muscovite, and the presence of goethite would be linked to the oxidation of ferromagnesian minerals (Ndjigui et al., 2013; Eko Bessa et al., 2018). A peculiarity is observed at Limbe beach, where most of the minerals appear, this could be due to the fact that the sediments of this sector are near to the volcanic line of Cameroon and the DSB.

The mineralogical data of sediments is consistent with the geochemical data (Tables 2 and 3). The abundance of quartz and kaolinite would be due to the high values of SiO<sub>2</sub>, Al<sub>2</sub>O<sub>3</sub>, and the moderate content of Fe<sub>2</sub>O<sub>3</sub> (Table 3). The content of Fe<sub>2</sub>O<sub>3</sub> refers to hematite/goethite. Illite is mainly composed of SiO<sub>2</sub>, Al<sub>2</sub>O<sub>3</sub>, and K<sub>2</sub>O. The presence of feldspars and plagioclase indicates the low abundance of MgO, K<sub>2</sub>O, Fe<sub>2</sub>O<sub>3</sub> and CaO. Sediments from Cameroon consist of quartz, clay minerals, heavy minerals, feldspars, ferric minerals and rock fragments. The presence of these minerals indicates that the

Table 3  
Major element concentrations of sediments compiled from various sites at Cameroon (wt. % oxides).

	Site 1	Site 2	site 3	site 4	site 5	site 6	site 7	site 8	site 9	site 10	site 11	site 12	site 13	site 14	site 15	site 16	site 17	site 18	site 19	site 20	site 21	site 22
SiO <sub>2</sub>	62.25	64.15	58.84	n.a.	—	48.21	41.71	67.45	66.70	46.70	69.48	46.70	25.34	32.01	80.11	78.55	84.90	87.32	51.34	62.40	88.84	31.4
Al <sub>2</sub> O <sub>3</sub>	16.46	17.32	16.88	n.a.	13.17	24.95	11.75	17.55	13.90	20.86	14.01	20.86	9.68	15.73	6.96	8.44	4.7	3.93	12.21	18.78	4.27	8.7
Fe <sub>2</sub> O <sub>3</sub>	6.77	4.21	3.43	n.a.	5.71	7.31	5.61	6.37	5.58	8.36	4.47	8.36	5.96	8.81	4.11	3.24	0.03	2.63	11.28	7.18	2.63	26.11
MgO	0.71	0.75	2.42	n.a.	4.59	0.02	4.81	0.2	0.06	1.47	0.21	0.63	0.6	0.29	0.47	0.21	0.08	0.15	0.86	2.19	0.17	10.95
CaO	0.4	0.07	1.91	n.a.	8.53	—	12.19	0.10	1.10	0.31	0.12	0.31	0.91	0.17	0.76	0.19	0.16	0.31	0.74	1.29	0.32	11.36
Na <sub>2</sub> O	0.2	0.13	1.36	n.a.	2.45	0.04	3.99	0.08	1.26	1.58	0.07	0.31	0.36	0.15	0.75	0.22	0.28	0.37	0.22	1.19	0.45	0.97
K <sub>2</sub> O	3.97	4.00	4.69	n.a.	4.02	0.2	1.86	0.3	1.23	0.63	0.6	1.58	0.63	0.62	2.35	0.80	0.25	0.4	0.74	3.68	1.55	0.32
TiO <sub>2</sub>	1.32	0.92	0.77	n.a.	0.57	1.37	0.56	1.89	1.93	0.06	1.63	1.47	1.73	3.21	2.61	1.07	1.04	1.37	3.44	0.99	0.56	6.37
P <sub>2</sub> O <sub>5</sub>	0.2	0.12	0.2	n.a.	0.35	0.06	0.20	0.12	0.63	0.31	0.2	0.23	0.23	0.26	0.07	0.08	0.03	0.01	0.36	0.16	0.05	0.43
MnO	0.04	0.13	0.15	n.a.	0.40	—	0.17	0.2	0.07	0.23	0.2	0.06	0.11	0.03	0.10	0.04	4.51	0.03	0.21	0.11	0.04	0.39
LOI	7.76	8.42	9.20	n.a.	—	17.2	16.82	4.44	6.78	2.25	8.22	18.85	54.17	38.01	2.11	6.91	2.5	3.25	19.95	6	1.02	2.7
Total	99.99	100.15	99.83	n.a.	—	99.31	99.70	99.10	99.30	99.44	99.12	99.44	99.71	99.3	100.41	99.75	98.84	99.84	99.99	103.97	99.88	99.4
SiO <sub>2</sub> /Al <sub>2</sub> O <sub>3</sub>	4.45	4.05	3.87	n.a.	—	2	4.80	3.84	5.20	2.23	5.85	2.25	2.61	2.06	12.01	10	19.28	26.51	4.20	3.32	20.80	3.8
K <sub>2</sub> O/Na <sub>2</sub> O	57.50	54.24	24.64	n.a.	1.64	5.00	0.47	3.75	0.97	5.33	8.57	5.33	1.75	4.13	3.13	3.55	0.86	1.14	3.36	3.09	3.62	0.34
Na <sub>2</sub> O/Al <sub>2</sub> O <sub>3</sub>	0.01	0.01	0.08	n.a.	0.2	0.001	22.59	0.004	0.1	0.07	0.004	0.01	0.04	0.01	0.11	0.02	0.06	0.1	0.02	0.06	0.10	0.1
Al <sub>2</sub> O <sub>3</sub> /TiO <sub>2</sub>	27.15	20.32	24.92	n.a.	23.10	18.21	14.66	9.28	7.20	14.55	8.59	14.55	5.59	4.95	3.79	7.88	4.51	3.00	3.55	19	7.62	1.76
Fe <sub>2</sub> O <sub>3</sub> /K <sub>2</sub> O	66.18	1.43	0.91	n.a.	1.42	36.55	2.27	21.23	4.53	13.26	7.45	5.29	9.46	16.06	1.74	5.2	65.23	6.3	15.24	1.95	0.11	140
CIA	79.80	78.45	65.00	n.a.	70.1	—	39.20	96.92	69.25	88.49	94.42	88.49	73.17	94.38	58	85.1	83	72.03	90.18	92.37	58.50	81
PIA	95.23	96.84	78.28	n.a.	81.2	—	38.87	98.70	73.03	94.93	98.45	94.93	92.63	97.88	64	92.5	85.66	76.21	94.45	71.36	65.39	82.3
CIW	97.00	97.94	82.96	n.a.	72.80	—	42.39	99.12	85.48	95.37	99.01	95.37	77.15	98.1	82.26	95.36	86.17	78.36	94.77	97.66	84.72	82.8

n.a. not analysed. - not identified.

sediments could come from a recycled orogeny, from a felsic, intermediate, and mafic sources. These results corroborate with the studies by Armstrong-Altrin et al. (2015) in Mexico, Abu and Sunkari (2020a, b) in Ghana, Ramamoorthy and Nazir (2020) in India.

#### 4.2. Major, trace and REE geochemistry

Twenty-one papers out of 22 reported geochemical analyzes. The results of these analyzes are given in Tables 3–5. Table 3, lists the concentrations of major elements of the selected sites. In this table, the SiO<sub>2</sub> concentrations are moderate (24.95–25.34 wt %) in DSB, Babouri-Figui, and Mayo Oulo-Lere basins, some rivers and lakes from the central and southern regions of the country. The Al<sub>2</sub>O<sub>3</sub> and Fe<sub>2</sub>O<sub>3</sub> contents are moderate to high (3.93–24.95 wt.%; 0.03–36.11 wt.%, respectively) for all sediment samples. The other elements have relatively low contents in all the sites. The values of the SiO<sub>2</sub>/Al<sub>2</sub>O<sub>3</sub> ratio varies between 2 and 20.8 (Table 3). Table 3 also presents the values of the alteration indices calculated at each site. The results of these indices are grouped and listed according to the regions highlighted in Table 1. The CIA presents moderate to very high values in the sediments of all the sites studied (65.00–96.92), except the sediments of the Sanaga river, Babouri-Figui and Mayo Oulo-Lere basin, and Mouanko beach (39.20–58.50) which has low CIA values (Table 3). The values of PIA and CIW have very high values in all the sites studied, the values of these indices vary from 81.2 to 98.70 for the PIA, and from 82.26 to 99.01 for CIW. Moderate PIA values (64–78.28) are observed in certain river sediments (Sanaga, Ngaye, and Dibamba), DSB, Mamfe basin, Kadey Plain, and Mouanko beach. Similarly, the sediments of Dibamba river, Ngaoundaba lake and Mamfe basin show moderate values of CIW (72.80–78.36). Moreover, the sediments of the Babouri-Figui and Mayo Oulo-Lere basins present low values in PIA (38.87) and CIW (42.39) Table 3. The SiO<sub>2</sub>/Al<sub>2</sub>O<sub>3</sub> ratio presents values lower than 3, these values indicate the predominance of clay-minerals. On the other hand, SiO<sub>2</sub>/Al<sub>2</sub>O<sub>3</sub> values ranging from 3 to 20.80, which indicate the predominance of quartz and kaolinite. The K<sub>2</sub>O/Na<sub>2</sub>O ratio values are ranging from 0.34 to 57.50.

Table 4 shows the trace element contents of the various sites studied. Barium contents are up to 100 ppm in all the sediments of studied regions. Zirconium contents range from 54 to 1883 ppm. Strontium, Cr, and V contents range from 20.5 to 650.3 ppm, 37.4–477.0 ppm and 31.3–743 ppm, respectively (Table 4), while Rb and Ni values range from 8.1 to 1900 ppm and 8.2–219.0 ppm, respectively. The other elements have contents lower than 100 ppm in all the sediments except sediments of Moloundou swamp, Mouanko and Limbe beach, which have Co, Sc, and Zn contents above 100 ppm (Table 4). The moderate to high contents in large-ion lithosphere elements (Rb, Sr, and Ba) suggest their incorporation in sheet silicates, such as illite and absorption on to clay mineral surfaces. The high to moderate concentrations of Sr in sediments may be due to the presence of feldspars.

Table 4

Trace element concentrations of sediments compiled from various sites at Cameroon (ppm).

	site 1	site 2	site 3	site 4	site 5	site 6	site 7	site 8	site 9	site 10	site 11	site 12	site 13	site 14	site 15	site 16	site 17	site 18	site 19	site 20	site 21	site 22
Ba	783.7	1057.2	1066.6	823.3	824.6	142.6	246.9	186.4	1016.9	1438.0	339.7	620.9	n.a.	184.3	852.9	435.0	137.5	252.9	—	650.0	566.9	257.0
Cr	128.3	59.0	42.1	68.2	68.2	125.9	62.2	237.0	96.6	81.4	148.6	127.4	n.a.	115.8	62.0	477.0	82.7	61.4	179.1	110.0	37.4	—
Zr	409.3	625.6	403.5	54.0	86.1	198.3	89.2	227.0	291.6	247.0	387.1	338.5	n.a.	52.7	1883.0	1253.0	663.6	743.3	385.8	210.0	329.5	428.0
Cs	3.2	2.4	3.7	—	—	1.8	0.5	0.5	1.9	1.3	3.1	n.a.	0.5	0.8	—	0.4	0.3	2.4	15.0	0.7	—	
Th	16.7	23.9	20.9	13.4	13.4	23.3	9.2	24.1	15.2	29.2	23.5	19.5	n.a.	8.9	25.2	23.9	10.8	20.4	—	14.6	5.6	15.7
U	3.2	4.7	4.6	36.1	4.0	2.9	1.2	2.8	1.1	4.7	3.1	4.4	n.a.	1.5	4.2	2.8	1.3	1.6	—	3.1	1.2	2.9
V	126.2	90.9	71.5	100.7	100.7	170.1	79.3	147.0	92.4	103.2	131.7	142.6	n.a.	77.3	70.7	46.8	71.3	52.3	311.8	150.0	31.3	743.0
Hf	10.8	21.3	10.0	—	2.0	5.9	2.5	6.4	7.3	6.4	10.2	8.2	n.a.	1.2	13.4	29.5	10.7	13.1	—	5.0	7.9	9.8
Nb	27.1	19.9	17.3	—	12.8	25.1	9.3	46.7	9.8	42.9	36.1	32.8	n.a.	10.6	43.7	13.9	21.4	19.8	—	1.9	12.5	145.0
Sr	197.7	294.5	331.6	376.8	376.6	49.9	650.3	20.5	184.9	100.5	39.6	102.4	n.a.	54.3	187.6	58.0	25.6	49.6	31.3	200.0	132.7	631.0
Y	34.0	36.3	30.9	20.12	20.1	15.8	26.9	10.8	16.3	11.8	19.5	33.5	n.a.	28.3	20.3	37.0	5.8	7.8	—	27.0	6.8	31.2
Ta	1.9	1.5	1.2	—	—	0.6	3.4	0.6	2.2	2.2	2.0	n.a.	0.0	3.1	0.8	1.4	1.3	—	—	0.9	10.8	
Ga	22.0	25.7	24.3	—	—	—	13.8	18.0	18.7	36.2	16.7	29.3	n.a.	14.9	—	10.1	6.8	6.1	—	—	4.5	25.0
Rb	122.4	118.6	134.9	—	259.1	8.9	47.9	10.2	55.4	25.2	22.8	38.7	n.a.	9.5	52.4	17.8	10.8	1900	—	160.0	39.0	8.1
Ni	54.3	25.5	39.6	38.6	38.6	37.7	35.7	17.2	42.9	38.2	36.0	52.4	n.a.	136.3	10.8	101.0	8.2	9.5	71.2	55.0	18.6	219.0
Co	13.5	10.5	13.4	23.7	23.7	17.1	11.9	13.6	18.3	7.3	25.1	25.9	n.a.	27.6	7.9	7.5	2.8	4.4	35.1	23.0	4.7	105.0
Cu	23.7	25.2	—	43.7	43.7	25.3	—	13.6	32.4	14.2	38.0	35.8	n.a.	51.5	9.3	—	12.1	6.6	193.1	50.0	—	—
Sc	12.2	8.4	9.2	11.7	11.7	20.0	10.8	9.9	11.5	8.8	12.5	16.3	n.a.	18.7	5.7	5.0	14.5	13.4	—	16.0	132.7	30.0
Pb	24.6	25.0	—	35.4	—	37.3	—	11.5	14.7	54.1	17.9	34.7	n.a.	12.6	18.2	—	10.5	8.1	18.7	20.0	—	—
Zn	56.0	53.0	—	94.0	94.0	24.2	—	43.8	55.8	72.9	83.6	90.3	n.a.	55.8	—	—	22.5	26.2	123.8	85.0	—	—
W	1.3	—	—	—	—	1.6	2.4	0.3	1.3	1.6	1.4	n.a.	0.0	1.5	—	0.9	0.3	—	—	1.0	—	
Sn	2.8	2.4	2.9	—	0.6	—	—	2.5	0.3	4.2	2.9	3.6	n.a.	1.7	—	—	—	—	3.7	—	—	2.8
Th/Co	2.9	2.3	4.2	0.6	—	1.4	0.7	1.8	0.8	4.0	0.9	0.8	n.a.	0.3	3.2	3.2	3.8	4.6	—	0.6	1.2	0.1

n.a. not analysed. - not identified.

Table 5

Rare earth elements (REE) element concentrations of sediments compiled from various sites at Cameroon (ppm).

	site 1	site 2	site 3	site 4	site 5	site 6	site 7	site 8	site 9	site 10	site 11	site 12	site 13	site 14	site 15	site 16	site 17	site 18	site 19	site 20	site 21	site 22
La	60.71	66.94	65.60	47.24	45.58	14.23	31.63	54.27	46.01	81.18	62.37	50.54	38.91	47.13	47.4	65.50	19.07	39.39	n.a.	42.96	12.91	152
Ce	120.15	130.38	127.70	92.87	89.45	34.70	63.03	114.64	91.16	140.68	137.01	114.15	83.05	–	97.57	132.00	48.26	77.45	n.a.	80.38	25.98	309
Pr	14.14	14.96	14.35	11.38	11.10	4.45	7.38	12.40	9.55	15.39	14.78	12.46	9.64	13.74	10.9	14.95	4.07	8.11	n.a.	9.51	2.63	34.79
Nd	53.19	54.75	52.96	41.62	40.48	17.69	28.55	46.78	34.47	50.15	55.38	45.40	32.23	53.74	40.21	53.50	14.29	27.72	n.a.	34.40	9.81	129
Sm	9.44	10.59	9.26	7.39	7.15	3.67	5.80	7.88	5.57	7.07	9.78	8.89	5.84	10.35	6.93	8.95	2.40	4.31	n.a.	6.38	1.68	17.7
Eu	2.26	2.13	1.94	1.63	1.45	0.77	1.19	0.86	1.2	1.35	1.32	1.99	1.62	3.04	0.86	0.91	0.29	0.39	n.a.	1.08	0.31	4.77
Gd	7.64	7.67	7.20	7.23	6.95	2.36	5.35	4.57	4.16	4.38	6.43	7.33	5.18	9.74	4.89	8.24	1.80	3.19	n.a.	5.50	1.34	12.17
Tb	1.06	1.02	1.02	0.88	0.85	0.27	0.85	0.48	0.55	0.57	0.74	1.07	0.81	1.22	0.64	1.10	0.00	0.00	n.a.	0.88	0.22	1.59
Dy	6.15	7.22	5.60	4.08	3.88	1.06	5.00	2.43	3.07	3.05	3.90	6.13	4.17	6.30	3.67	6.44	1.12	1.58	n.a.	5.49	1.16	7.39
Ho	1.14	1.39	1.06	0.68	0.63	0.15	1.02	0.42	0.57	0.52	0.71	1.21	0.79	1.04	0.73	1.37	0.22	0.30	n.a.	1.13	0.25	1.24
Er	3.21	3.76	3.04	1.92	1.78	0.29	2.97	1.16	1.63	1.34	2.02	3.45	1.87	2.74	2.24	4.08	0.63	0.78	n.a.	3.39	0.75	3.08
Tm	0.44	0.46	0.42	0.24	0.20	0.03	0.41	0.17	0.23	0.17	0.29	0.51	0.29	0.00	0.35	0.64	0.00	0.00	n.a.	0.51	0.12	0.42
Yb	2.74	3.15	2.80	1.52	1.43	0.20	2.50	1.13	1.52	1.05	1.96	3.25	2.02	2.00	2.6	3.86	0.74	0.83	n.a.	3.41	0.88	2.57
Lu	0.40	0.46	0.42	0.22	0.20	0.03	0.36	0.17	0.23	0.14	0.29	0.47	0.26	0.00	0.41	0.64	0.13	0.18	n.a.	0.52	0.14	0.34
LREE	282.70	304.87	293.36	218.89	211.10	79.88	156.04	247.34	199.66	307.1	296.95	256.82	186.66	221.87	203.01	302.00	93.02	164.25	n.a.	195.51	58.19	677
HREE	259.90	279.74	271.80	209.35	202.15	75.51	142.93	236.82	184	295.8	287.08	233.42	171.28	195.17	218.84	284.50	88.43	157.35	n.a.	173.62	53.34	645
$\Sigma$ HREE	22.80	25.13	21.56	29.54	8.95	4.37	13.11	10.52	15.66	11.23	9.90	23.41	15.38	12.83	15.56	18.00	4.63	6.85	n.a.	20.81	4.85	28.8
LREE/HREE	12.28	12.0–2	12.71	7.21	22.35	23.56	11.82	22.50	11.75	26.35	32.80	9.89	11.05	15.54	11.9	15.00	15.86	21.10	n.a.	9.89	11.04	23
Eu/Eu*(1)	1.25	1.10	1.11	0.45	0.64	1.22	1.00	0.54	0.76	0.74	0.50	0.75	0.86	1.41	0.55	0.43	0.57	0.51	n.a.	0.58	1.02	1.1
Eu/Eu*(2)	1.25	1.11	1.11	0.60	0.96	0.61	0.84	0.67	1.2	1.13	0.78	1.15	1.38	1.4	0.76	0.49	0.66	0.48	n.a.	0.85	0.93	1.5
Eu/Eu*(3)	1.24	1.13	1.13	1.19	1.63	0.79	1.04	0.76	1.16	1.14	0.51	0.75	0.90	0.92	0.45	0.32	0.42	0.31	n.a.	0.63	0.79	0.19
(La/Yb)N	1.79	1.64	1.77	1.50	20.61	5.05	1.01	34.03	2.43	5.71	25.61	10.53	13.51	12	11.53	11.26	16.35	30.23	n.a.	11.42	10.46	15.57
La/Sc	6.78	30.49	–	4.24	4.24	0.71	2.92	5.46	3.99	9.24	5	3.11	–	2.54	18.2	14.18	2.0	–	n.a.	2.77	4.72	0.5
La/Th	4.73	2.48	3.54	3.99	3.4	0.61	3.45	2.24	3.03	2.77	2.65	2.3	–	5.28	1.88	2.99	1.77	4.09	n.a.	2.94	2.53	2.69
La/Yb	22.15	21.25	23.43	31.54	30.92	71.15	5.69	48.02	30.26	77.31	31.82	15.55	19.26	23.56	18.23	16.96	25.77	48.06	n.a.	12.59	15.48	59.14

n.a. not analysed. – not identified.

**Table 5** shows the contents of rare earth elements (REE) at each site studied. In the context of this work, the majority of the sites studied show high contents of Ce (25.98–309 ppm), La (19.07–152 ppm), and Nd (14.29–129 ppm). The praseodymium values obtained are mostly moderate in all the sites, which vary from 12.46 to 34.79 ppm. The contents of other elements show values below 10 ppm at all sites (**Table 5**). In all the sites the abundance of ΣREE is low and varies from (4.37–29.54), with a relatively higher abundance LREE (58.19–677) than HREE (53.34–645). LREE/HREE ratio of sediments at all sites range between 9.89 and 32.80, these values revealed that the sediments in Cameroon are more enriched in LREE. On PAAS, UCC and chondrite-normalized REE patterns, slight positive Eu anomalies are observed for at most sites ( $\text{Eu/Eu}^* = 0.19\text{--}1.41$ ,  $0.60\text{--}1.5$ , and  $0.19\text{--}1.63$ , respectively). High to moderate values of  $(\text{La/Yb})_N$  is observed, ranging between 5.05 and 34.03 in most sites (**Table 5**). These values reflect the combination of sediments derived from heterogenous source rocks during weathering processes.

## 5. Discussion

### 5.1. Classification of sediments

In the Herron diagram ([Herron, 1988](#)), the sediments of Cameroon are classified into several domains especially Fe-

shale, shale, Fe-sand, wacke, arkose, litharenite, sub-litharenite and quartzarenite ([Fig. 3](#)). In short, the sediments which come from sedimentary basins are classified as shale, Fe-shale, Fe-sand, arkose, and wacke ([Fig. 3](#)). Sediments from rivers (Mefou, Ngaye and Lokoundje), and lakes (Ossa, Ngaoundaba and Fonjak) are plotted in the shale, Fe-shale and shale fields. Recent sediments (Simbock Lake) are classified as Fe-Sand and litharenite as well as the sediments of the biggest rivers that flow directly into the Atlantic Ocean (Sanaga, Nyong, Dibamba and Lobe). The sediments of swamp, plain and beaches near the volcanic line areas of Cameroon are classified as Shale, Fe-sand and wacke. While, those from other beaches are classified as sublitharenite ([Fig. 3](#)). Furthermore, the sediments that fall in the field of Fe-sand and quartz arenite suggests that these sediments originate from granitic and Fe-bearing bedrock and also reflects the presence of quartz and feldspars in the sediments, indicating the predominance of felsic and mafic sources ([Abu and Sunkari, 2020a, 2020b](#)). Likewise, the arkose and sublitharenite would be due to the abundance of rock fragments and feldspars.

### 5.2. Weathering and nature of source rocks

**Table 3** reports three weathering indices (CIA, PIA and CIW). The chemical index of weathering values of the studied sediments shows that, the values of the samples from all these

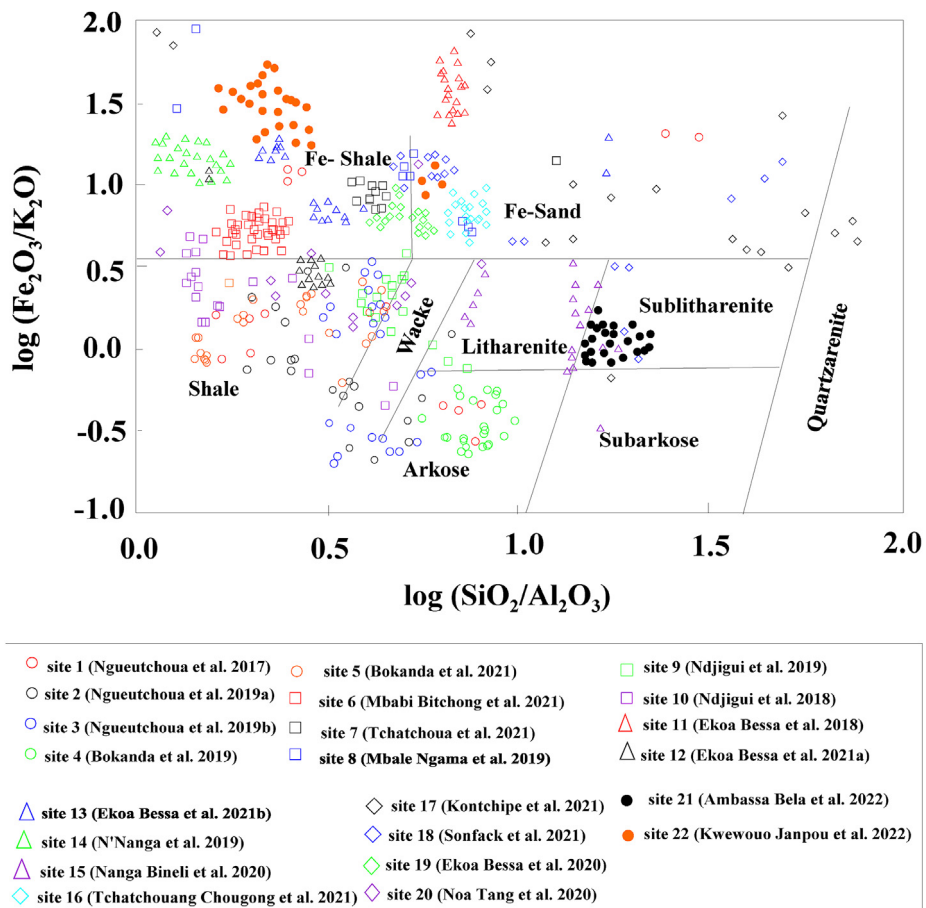


Fig. 3. Geochemical classification of the Cameroon's sediments, using  $\log(\text{Fe}_2\text{O}_3/\text{K}_2\text{O})$  vs  $\log(\text{SiO}_2/\text{Al}_2\text{O}_3)$  diagram (after [Herron, 1988](#)).

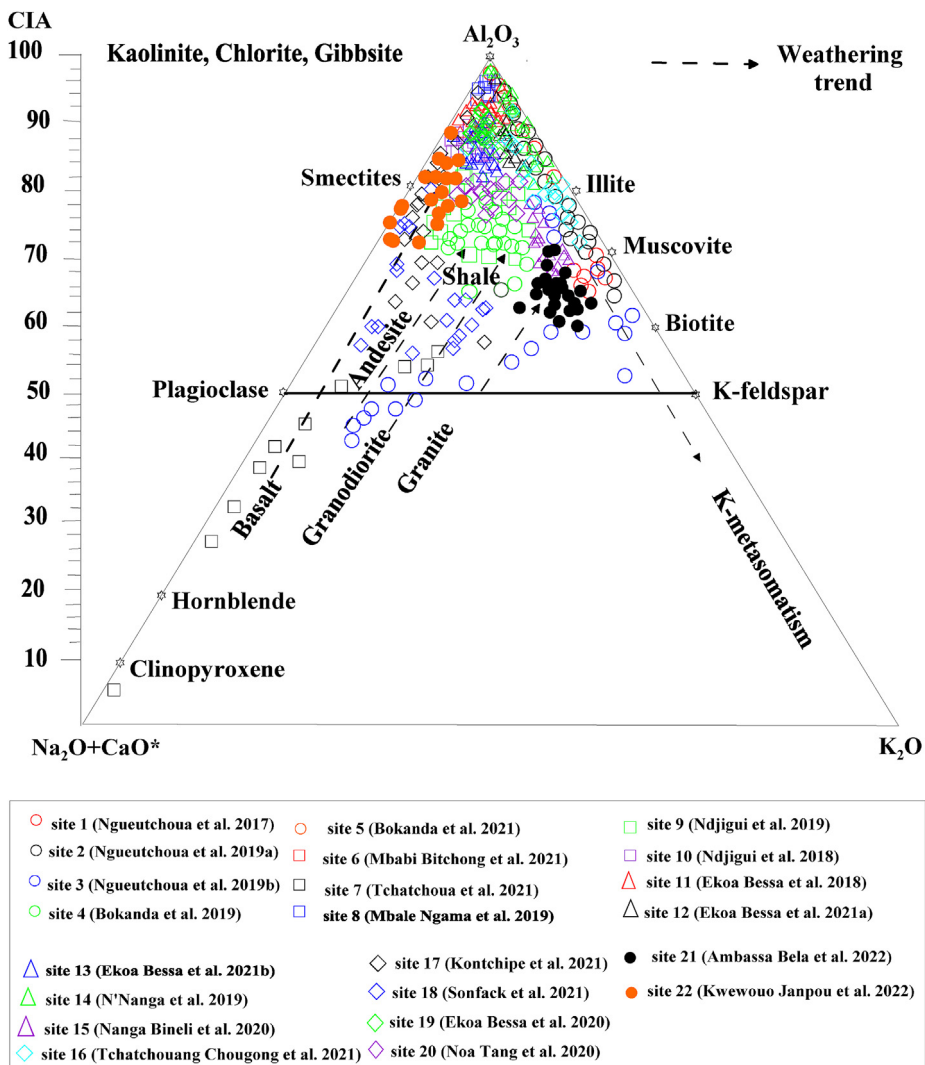


Fig. 4. Ternary diagram showing the weathering conditions of the studied sediments: A-CN-K (after Nesbitt and Young, 1982).

sites ranges between 60 and 80, and >80, which indicates that the sediments of this zone would have undergone a moderate to strong weathering intensity. Moreover, the sediments from the northern region of the country, the biggest rivers, and the meridional sand beaches presents a low to moderate degree of alteration. It is in accordance with the values of CIA, which indicate strong and moderate weathering of the source rocks as it is excepted in equatorial area (Liu et al., 2016) as well as the siliciclastic nature of sediments (Fedo et al., 1995). The PIA and CIW values reflect the intense feldspars alteration (Fedo et al., 1997; Mbale Ngama et al., 2019). The enrichment of the K<sub>2</sub>O/Na<sub>2</sub>O ratio (0.34–57.50) implies plagioclase disintegration as K-feldspar during weathering (Gu et al., 2002; Armstrong-Altrin et al., 2015, 2022) and/or K-reintroduction in the system during diagenesis (Madhavaraju and Lee, 2010; Madhavaraju, 2015).

Fig. 4, presents the distribution of oxides in the ternary diagram A-CN-K. The present study shows that the samples from all stations are positioned above the K-feldspars and plagioclase line, with the exception of certain samples from

sedimentary basin which are below this line. This diagram shows that plagioclases are more easily dissolved than K-feldspars, therefore the sample positions are most likely due to the differential dissolution of labile minerals. It's also possible that K<sub>2</sub>O was added to the aluminous clay during the diagenesis process. The position of samples near different minerals (Fig. 4) confirms the mineralogical assemblage obtained by the XRD data (Table 2). This result shows that the sediments from Cameroon derived from several source rocks (igneous, metamorphic and sedimentary) including basalt, gneiss, granite, granodiorite and shale, which is confirmed by the geology of each region mentioned in this study.

### 5.3. Provenance

Concentrations of major elements, such as Al<sub>2</sub>O<sub>3</sub> and TiO<sub>2</sub>, as well as trace elements (i.e., Hf, Th, Sc, Cr, Zr, Ni, V, and Co), REE and mineralogy in clastic sediments are commonly used to infer the provenance of sedimentary clastic rocks, because they tend to reflect the source rock (Madhavaraju et al.,

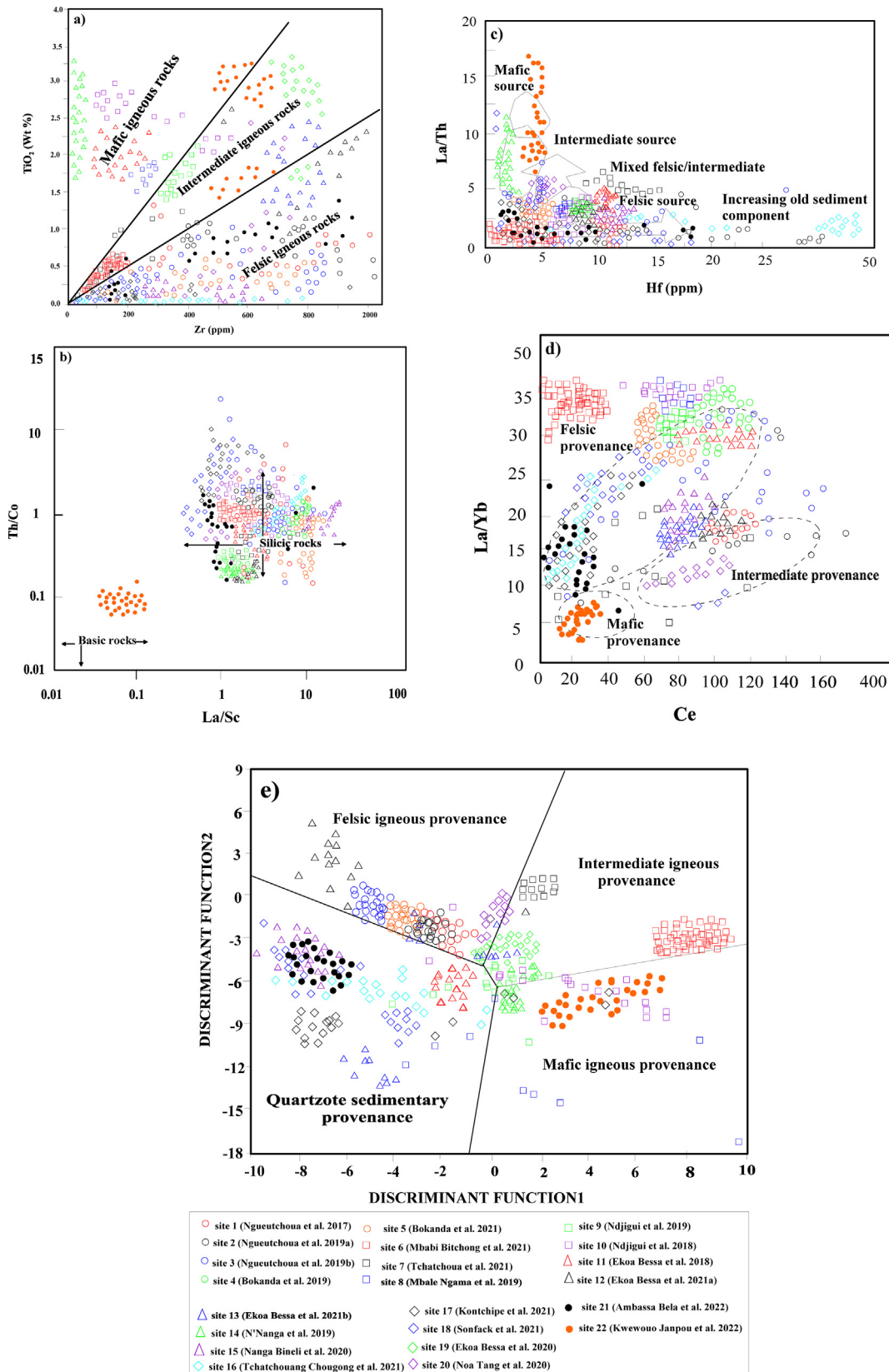


Fig. 5. Bivariate plots for the samples from sites studied: a)  $\text{TiO}_2$  versus Zr (after Hayashi et al., 1997), b) La/Sc vs Th/Co (after Cullers, 2000), c) Hf vs La/Th (after Floyd and Leveridge, 1987), d) Ce vs La/Yb (after Rao et al., 2011), e) Discriminant function plot of Roser and Korsch (1988). The discriminant functions are: Discriminant Function 1 =  $(-1.773 * \text{TiO}_2) + (0.607 * \text{Al}_2\text{O}_3) + (0.760 * \text{Fe}_2\text{O}_3) + (-1.500 * \text{MgO}) + (0.616 * \text{CaO}) + (0.509 * \text{Na}_2\text{O}) + (-1.224 * \text{K}_2\text{O}) + (-9.090)$ ; Discriminant Function 2 =  $(0.445 * \text{TiO}_2) + (0.070 * \text{Al}_2\text{O}_3) + (0.250 * \text{Fe}_2\text{O}_3) + (-1.142 * \text{MgO}) + (0.438 * \text{CaO}) + (1.475 * \text{Na}_2\text{O}) + (-1.426 * \text{K}_2\text{O}) + (-6.861)$ .

2016; Verma and Armstrong-Altrin, 2016; Anaya-Gregorio et al., 2018; Ramírez-Montoya et al., 2022). The REE pattern and the extent of the Eu anomaly can be used to depict the source rock (Etemad-Saeed et al., 2011; Armstrong-Altrin et al., 2004; 2016; 2021b). The minerals identified on the XRD, in particular: quartz, clay minerals, heavy minerals, feldspars and rock fragments indicates that the sediments of the Cameroonian zone could come from a recycled orogeny, felsic, intermediate, and mafic source. These results corroborate those of Armstrong-Altrin et al. (2015) in Mexico, Abu and Sunkari (2020a, b) in Ghana, Ramamoorthy and Nazir (2020) in India. The geochemical data of sediments from Cameroon has been presented in a series of binary diagrams, which are often used in provenance investigations to determine the composition of their source rock (Fig. 5). Hayashi et al. (1997) proposed a binary diagram of Zr vs TiO<sub>2</sub> that has been used by various authors in sedimentary provenance study. This diagram can be used to identify mafic rocks ( $\text{TiO}_2/\text{Zr} > 200$ ), intermediate rocks ( $\text{TiO}_2/\text{Zr}$  ranging between 55 and 200), and felsic igneous rocks ( $\text{TiO}_2/\text{Zr} < 55$ ). In this study, most of the samples from the selected sites are plotted in the igneous felsic rocks field. The sediments from small rivers and lakes from the Center of the Cameroon fall exclusively in the domain of mafic igneous rocks. The sediments from big rivers fall in the mafic and intermediate igneous domain. On this diagram, the sediments from rivers and lakes at Adamawa and those from the beaches near the volcanic lines fall mainly in the field of intermediate igneous and mafic rocks (Fig. 5a). By grouping these data, it seems that the sediments of southwest and those of the Adamawa Region come from felsic, mafic and intermediate igneous sources, the origin of these sediments differs from sediments studied in India by Tiju et al. (2018), and those of Saudi Arabia by Bantan et al. (2020). Sediments in the South come mostly from felsic sources, these sediments are compared with sediments of floodplain in Southern Kerala, India (Tiju et al., 2018), and those in the Central region come mainly from mafic sources. The sediments in the North come from mafic and intermediate igneous sources, these sediments are similar to those in Saudi Arabia by Bantan et al. (2020). While those of the eastern coast come from felsic and intermediate igneous sources, these sediments are compared with those of estuarine sediments in southern Kerala, India (Tiju et al., 2018).

Source composition can be determined using elemental ratios such as Th/Co, La/Sc, and Th/Co vs La/Sc bivariate plot (Cullers, 2000). The values of Th/Co (0.67–19.4) and La/Sc (2.50–16.3) are suggestive of felsic source, while those of Th/Co (0.04–1.4) and La/Sc (0.43–0.86) are indicative of mafic source. In this study, Th/Co (0.35–4.60) and La/Sc (2.00–30.49) indicate mostly felsic source rocks for all the sites except the site of Limbe beaches near volcanic line of Cameroon, which indicate mafic source rocks. This result is showed in the Th/Co vs La/Sc diagram, where all the samples of the different sites plotted around the field of felsic igneous rocks, except the site of Limbe beaches, which shows that these samples plot in the field of mafic igneous rocks (Fig. 5b). Furthermore, high zircon concentrations (up to 1883.0 ppm)

imply granitic or recycled detrital rock sources (Carranza-Edwards et al., 2001).

The La/Th vs Hf (Fig. 5c; Floyd and Leveridge, 1987) and La/Yb vs Ce (Rao et al., 2011, Fig. 5d) plots are used to differentiate mafic from felsic pristine rocks. The La/Th vs Hf binary diagram shows that sediment particles of all sites derived from a source area composed of intermediate, mixed felsic/intermediate and felsic rocks. This diagram further reveals the presence of old sediment components represented by samples of Southwest (DSB) and Lobe river in the South. Moreover, the samples plot in the field of mafic and intermediate sources. This result is consistent with the presence of possible Pan African metasediments. In the La/Yb vs Ce diagram, all the samples from the different sites are close to the field of felsic and intermediate provenance. Except the sediments of Limbe beaches near the volcanic line which fall in the field of mafic provenance.

A number of studies (e.g., Nagarajan et al., 2007; Etemad-Saeed et al., 2011; Zaid, 2012; Ramos-Vázquez et al., 2022) have inferred the source rock composition of sedimentary clastic rocks using the discriminant function diagram proposed by Roser and Korsch (1988), this diagram discriminates four possible sources of sediments: mafic, felsic, intermediate, and quartzose sedimentary origin (Fig. 5e). According to this diagram, the sediments of the various studied sites plotted on either side of the four groups. This diagram reveals that the sediments from Kadey plain, and Ossa lake are derived from igneous felsic provenance. This felsic provenance may be linked to gneisses, pre- Pan African granitoids, and volcanic rocks (Eko Bessa et al., 2021a, 2021b). Samples studied from sedimentary basins, rivers from the Adamawa, and the swamp in the East, derived from intermediate igneous provenance (Fig. 5e). This intermediate provenance is attributed to the mixture of gneisses, metasediments and amphibolites located near to the study area, it also indicates that sediments derived from the mixed provenance (Eko Bessa et al., 2021a). The sediments of numerous rivers (Mefou, Sanaga, Lobe, Nyong and Dibamba), some lakes (Simbock and Ngaoudaba), and beaches in the meridional littoral of Cameroon derived from quartzose sedimentary provenance (Fig. 5e). This quartzose sedimentary origin linked to acidic rocks (Nanga Bineli et al., 2020). This indicates the predominance of mature polycyclic siliciclastic rocks, with subordinate contribution from first cycle basic and felsic rocks (Kontchipe et al., 2021; Sonfack et al., 2021). The sediments from volcanic line of Cameroon derived from mafic igneous provenance (Fig. 5e). This mafic provenance is made up of Tertiary formations with also amphibolites, pyroxenites, and amphibolite gneisses (Lerouge et al., 2006).

## 6. Conclusion and recommendations

The following conclusions can be drawn from this work.

1. The sediments from Cameroon (Central Africa) consist of quartz, feldspar, clay minerals, heavy minerals, ferric minerals and rocks fragments. These sediments mainly

- consist of  $\text{SiO}_2$ ,  $\text{Al}_2\text{O}_3$ , and  $\text{Fe}_2\text{O}_3$  in high amount, they are rich in some trace elements (Ba, Zr, Sr, Cr, and V), rich in silica and light rare earths (LREE).
2. Cameroon's sediments are classified as Fe-shale, shale, Fe-sand, wacke, arkose, litharenite, sublitharenite and quartzarenite. The weathering indexes, as well as A-CN-K ternary diagram show mostly moderate and strong weathering of the rock sources. Likewise, the result of nature of source rocks show that sediments of Cameroon derived from several source rocks including Tertiary and recent basalts, gneisses, granitoids, recent sediments and Phanerozoic cover.
  3. These databases represent the first national survey on the provenance of sediments in Cameroon, and we except that these results will be useful for future work to infer the depositional environments. Moreover, it can also make it possible to identify the zone which have a high concentration of placer deposits and sediments enriched in trace elements, which is important to facilitate their exploration.

## Funding

AZEB testifies on behalf of all the authors of this paper that, this research has not received any specific grant from any funding body in the public, commercial or non-profit sectors. JSAA participated in this work during the sabbatical period at the Bharathidasan University, which was approved by DGAPA (PASPA), UNAM.

## Author's contribution

All the authors quoted in this paper have participated ardently in the writing of this manuscript, by exposing very beneficial arguments in the context of this study and have also worked for the form and the linguistic quality provide in this document.

## Ethics approval and consent to participate

For the time being, AZEB consciously ensures that the following conditions are met for the manuscript “*Provenance of clastic sediments: A case study from Cameroon, Central Africa*”: (1) the data and materials used in this paper are not the original work of the first author, but rather a compilation of the works of several previously published articles; (2) the paper is not considered for publication elsewhere; (3) the work essentially reflects the research and analysis data of compiled from the previous work of several authors; (4) the results are appropriately placed in the context of previous research; (5) all sources used are properly disclosed; (6) all authors have been actively involved in substantial work leading the document and will bear public responsibility for its contents. Thereafter we indicate our consent to participate in the research, and we add that the compilation of the data carried out in this study will be used specifically for a doctoral

work of the first author and will also be used under abstract form for publication of reviews, and we consent to its use in this manner. We agree with the statements above and declare that this submission follows the policies of *Solid Earth Sciences* as outlined in the guide.

## Consent for publication

We, the undersigned, agree to the publication of identifiable details, which may include figures and details in the text to be published in the *Solid Earth Sciences*. We understand that all Springer journals may be available in both print and on the internet, and be accessible to a wider audience through marketing channels and other third parties. Therefore, anyone can read the documents published in the newspaper.

## Availability of data and materials

All data used in this study have been reported in tables (1–5). The methodology used in this study is that used by the authors of the various articles used and a compilation of these studies. We add that no additional data was carried out for the realization of this work.

## Declaration of competing interest

The authors declare that they have no known competing financial interests or personal relationships that could have appeared to influence the work reported in this paper.

## Acknowledgment

The authors are grateful to the sedimentology crew and the Laboratory of Geosciences of superficial Formation and Applications of the Department of Earth Sciences, University of Yaoundé I.

## References

- Abu, M., Sunkari, E.D., 2020a. Geochemistry and petrography of beach sands along the western coast of Ghana: implications for provenance and tectonic settings. *Turk. J. Earth Sci.* 29, 363–380. <https://doi.org/10.3906/yer-1903-8>.
- Abu, M., Sunkari, E.D., 2020b. Geochemistry, grain size characterization and provenance of beach sands along the central coast of Ghana. *Adv. Res. Chem. Appl. Sci.* 2, 15–26.
- Anaya-Gregorio, A., Armstrong-Altrin, J.S., Machain-Castillo, M.L., Montiel-García, P.C., Ramos-Vázquez, M.A., 2018. Textural and geochemical characteristics of late Pleistocene to Holocene fine-grained deep-sea sediment cores (GM6 and GM7), recovered from southwestern Gulf of Mexico. *J. Palaeogeogr.* 7, 1–19. <https://doi.org/10.1186/s42501-018-0005-3>.
- Armstrong-Altrin, J.S., 2020. Detrital zircon U-Pb geochronology and geochemistry of the Riachuelos and Palma Sola beach sediments, Veracruz State, Gulf of Mexico: a new insight on palaeoenvironment. *J. Palaeogeogr.* 9, 1–27. <https://doi.org/10.1186/s42501-020-00075-9>.
- Armstrong-Altrin, J.S., Machain-Castillo, M.L., 2016. Mineralogy, geochemistry, and radiocarbon ages of deep sea sediments from the Gulf of Mexico. *Mexico J. S. Am. Earth Sci.* 71, 182–200. <https://doi.org/10.1016/j.jsames.2016.07.010>.
- Armstrong-Altrin, J.S., Lee, Y.I., Verma, S.P., Ramasamy, S., 2004. Geochemistry of sandstones from the upper Miocene Kudankulam

- Formation, Southern India: implications for provenance, weathering, and tectonic setting. *J. Sediment. Res.* 74, 285–297. <https://doi.org/10.1306/082803740285>.
- Armstrong-Altrin, J.S., Nagarajan, R., Lee, Y.I., Kasper-Zubillaga, J.J., Córdoba-Saldaña, L.P., 2014. Geochemistry of sands along the San Nicolás and San Carlos beaches, Gulf of California, Mexico: implications for provenance and tectonic setting. *Turk. J. Earth Sci.* 23, 533–558. <https://doi.org/10.3906/yer-1309-21>.
- Armstrong-Altrin, J.S., Nagarajan, R., Balaram, V., Natalhy-Pineda, O., 2015. Petrography and geochemistry of sands from the Chachalacas and Veracruz beach areas, western Gulf of Mexico, México: constraints on provenance and tectonic setting. *J. S. Am. Earth Sci.* 64, 199–216. <https://doi.org/10.1016/j.jsames.2015.10.012>.
- Armstrong-Altrin, J.S., Alfonso, V., Botello, A.V., Villanueva, S.F., Soto, L.A., 2019. Geochemistry of surface sediments from the northwestern Gulf of Mexico: implications for provenance and heavy metal contamination. *Geol. Q.* 63, 522–538. <https://doi.org/10.7306/gq.1484>.
- Armstrong-Altrin, J.S., Ramos-Vázquez, M.A., Hermenegildo-Ruiz, N.Y., Madhavaraju, J., 2021a. Microtexture and U-Pb geochronology of detrital zircon grains in the Chachalacas beach, Veracruz State, Gulf of Mexico. *Geol. J.* 56, 2418–2438. <https://doi.org/10.1002/gj.3984>.
- Armstrong-Altrin, J.S., Madhavaraju, J., Vega-Bautista, F., Ramos-Vázquez, M.A., Pérez-Alvarado, B.Y., Kasper-Zubillaga, J.J., Eko Bessa, A.Z., 2021b. Mineralogy and geochemistry of Tecolutla and Coatzacoalcos beach sediments, SW Gulf of Mexico. *Appl. Geochem.* 134, 105103. <https://doi.org/10.1016/j.apgeochem.2021.105103>.
- Armstrong-Altrin, J.S., Ramos-Vázquez, M.A., Madhavaraju, J., Marca-Castillo, M.E., Machain-Castillo, M.L., Márquez-García, A.Z., 2022. Geochemistry of marine sediments adjacent to the Los Tuxtlas volcanic complex, Gulf of Mexico: constraints on weathering and provenance. *Appl. Geochem.* 141, 105321. <https://doi.org/10.1016/j.apgeochem.2022.105321>.
- Asaah, A.V., Zoheir, B., Lehmann, B., Frei, D., Burgess, R., Suh, C.E., 2014. Geochemistry and geochronology of the ~620 Ma gold-associated Batouri granitoids, Cameroon. *Int. Geol. Rev.* 57, 1485–1509. <https://doi.org/10.1080/00206814.2014.951003>.
- Banerji, U.S., Dubey, C.P., Goswami, V., Joshi, K.B., 2022. Geochemical indicators in provenance Estimation. In: Armstrong-Altrin, J.A., Pandarinath, K., Verma, S. (Eds.), *Geochemical Treasures and Petrogenetic Processes*, pp. 95–121. [https://doi.org/10.1007/978-981-19-4782-7\\_5](https://doi.org/10.1007/978-981-19-4782-7_5).
- Bantan, R.A., Ghandour, I.M., Aaid, G., Al-Zubieri, 2020. Mineralogical and geochemical composition of the subsurface sediments at the mouth of Wadi Al-Hamid, Red Sea coast, Saudi Arabia: implication for provenance and climate. *Environ. Earth Sci.* 79, 1–20. <https://doi.org/10.1007/s12665-019-8787-x>.
- Biwolé, A.B., Morin-Rivat, J., Fayolle, A., Bitondo, D., Dedry, I., Dainou, K., Doucet, J.L., 2015. New data on the recent history of the littoral forests of southern Cameroon: an insight into the role of historical human disturbances on the current forest composition. *Plant Ecol. Evol.* 148, 19–28. <https://doi.org/10.5091/plecevo.2015.1011>.
- Bokanda, E.E., Fralick, P., Ekomané, E., Njilah, I.K., Bissey, S.B., Akono, D.F., Eko Bessa, A.Z., 2019. Geochemical characteristics of shales in the Mamfe Basin, South West Cameroon: implication for depositional environments and oxidation conditions. *J. Afr. Earth Sci.* 149, 131–142. <https://doi.org/10.1016/j.jafrearsci.2018.08.004>.
- Bokanda, E.E., Fralick, P., Ekomané, E., Ntoboh, T.C., Nkongho, A.E., Belinga Belinga, C., 2021. Geochemical constraints on the provenance, paleoweathering and maturity of the Mamfe black shales, west Africa. *J. Afr. Earth Sci.* <https://doi.org/10.1016/j.jafrearsci.2020.104078>.
- Bouyo, H.M., Toteu, S.F., deloule, E., Penaye, J., Van Schmus, W.R., 2009. U-Pb and Sm-Nd dating of high-pressure granulites from Tchollire and Banyo regions: evidence for a Pan-African granulite facies metamorphism in north-central Cameroon. *J. Afr. Earth Sci.* 54, 144–154. <https://doi.org/10.1016/j.jafrearsci.2009.013>.
- Bouyo, M.H., Penaye, J., Njel, U.O., Moussango, A.P.I., Sep, J.P.N., Nyama, B.A., Wu, F., 2016. Geochronological, geochemical and mineralogical constraints of emplacement depth of TTG suite from the Sinassi Batholith in the Central African Fold Belt (CAFBB) of northern Cameroon: implications for tectonomagmatic evolution. *J. Afr. Earth Sci.* 116, 9–41. <https://doi.org/10.1016/j.jafrearsci.2015.12.005>.
- Brito de Neves, B.D., Van schmus, W.R., Fetter, A., 2001. North Western Africa-North Eastern Brazil: major tectonic links and correlations problems. *J. Afr. Earth Sci.* 34, 275–278. [https://doi.org/10.1016/S0899-5362\(02\)00025-8](https://doi.org/10.1016/S0899-5362(02)00025-8).
- Carranza-Edwards, A., Centeno-García, L., Rosales-Hoz, L., Lozano-Santa Cruz, R., 2001. Provenance of beach gray sands from western Mexico. *J. S. Am. Earth Sci.* 14, 291–305. [https://doi.org/10.1016/S0895-9811\(01\)00028-1](https://doi.org/10.1016/S0895-9811(01)00028-1).
- Chaplain, M., 2019. *Dynamique des matières en suspension en mer côtière : Caractérisation, quantification et interactions sédiments/matière organique*. Thèse de doctorat, Brest.
- Chougong Tchatchouang, D., Eko Bessa, A.Z., Ngueutchoua, G., Fouateu Yongue, R., Carole Nyam, S., Armstrong-Altrin, J.S., 2021. Mineralogy and geochemistry of Lobe River sediments, SW Cameroon: implications for provenance and weathering. *J. Afr. Earth Sci.* 1–19. <https://doi.org/10.1016/j.jafrearsci.2021.104320>.
- Cojan, I., Renard, M., 2021. *Sédimentologie 3<sup>e</sup> éd.* Dunod.
- Cullers, R.L., 1994. The controls on the major and trace element variation of shales, siltstones and sandstones of Pennsylvanian e Permian age from uplifted continental blocks in Colorado to platform sediment in Kansas, USA. *Geochem. Cosmochim. Acta* 58, 4955–4972. [https://doi.org/10.1016/0016-7073\(94\)90224-0](https://doi.org/10.1016/0016-7073(94)90224-0).
- Cullers, R.L., 2000. The geochemistry of shales, siltstones and sandstones of Pennsylvanian -Permian age, Colorado, U.S.A.: implications for provenance and metamorphic studies. *Lithos* 51, 181–203. [https://doi.org/10.1016/S0024-4932\(99\)00063-8](https://doi.org/10.1016/S0024-4932(99)00063-8).
- Donfack, P., 2011. Chapitre 8 changement climatique et faune sauvage en Afrique de l'Ouest et du Centre. Forêts, faune sauvage et changement climatique en Afrique, p. 163.
- Doum, J.M., Fuh, G.C., Fadil-Djenabou, S., Onana, V.L., Ndjigui, P.D., Armstrong-Altrin, J.S., 2020. Characterization and potential application of gleysols and ferralsols for ceramic industry: a case study from Dimako (Eastern Cameroon). *Arab. J. Geosci.* 13, 1–21. <https://doi.org/10.1007/s12517-020-06007-0>.
- Eko Bessa, A.Z., Ngueutchoua, G., Ndjigui, P.D., 2018. Mineralogy and geochemistry of sediments from Simbock Lake, Yaoundé area (southern Cameroon): provenance and environmental implications. *Arab. J. Geosci.* 11, 710. <https://doi.org/10.1007/s12517-018-4061-x>.
- Eko Bessa, A.Z., Ngueutchoua, G., Ekomane, E., Bissé, S.B., Bokanda, E.E., Chougong, D., Kam, J.A., Tessontsap, T., 2020. Provenance and weathering conditions of the Moloundou swamp sediments, southeast Cameroon: Evidence from mineralogy and geochemistry. *Solid Earth Sciences* 1–13. <https://doi.org/10.1016/j.secsci.2020.06.002>.
- Eko Bessa, A.Z., Ndjigui, P.-D., Gentry, C.F., Selvamony, J., Armstrong-Altrin, J.S., Bineli Betsi, T., 2021a. Mineralogy and geochemistry of the Ossa lake Complex sediments, Southern Cameroon: Implications for paleoweathering and provenance. *Arab. J. Geosci.* 14, 322. <https://doi.org/10.1007/s12517-021-06591-9>.
- Eko Bessa, A.Z., Armstrong-Altrin, J.S., Gentry, C.F., Bineli Betsi, T., Tebogo, K., Ndjigui, P.-D., 2021b. Mineralogy and geochemistry of the Ngaoundaba Crater Lake sediments, northern Cameroon: implications for provenance and trace metals status. *Acta Geochim.* 40, 718–738. <https://doi.org/10.1007/s11631-021-00463-5>.
- Eko Bessa, A.Z., Ambassa Bela, V., Ngueutchoua, G., et al., 2022. Characteristics and Source Identification of Environmental Trace Metals in Beach Sediments Along the Littoral Zone of Cameroon. *Earth Syst. Environ.* 6, 175–187. <https://doi.org/10.1007/s41748-021-00279-6>.
- El Houssainy, A., 2020. *Apports de géochimie sédimentaire des éléments traces métalliques dans deux zones côtières méditerranéennes urbanisées : Beyrouth (Liban) et Toulon (France)*. Doctoral dissertation, Université de Toulon.
- Etemad-Saeed, N., Hosseini-Barzi, M., Armstrong-Altrin, J.S., 2011. Petrography and geochemistry of clastic sedimentary rocks as evidence for provenance of the Lower Cambrian Lalun Formation, Posht-e-badam block, Central Iran. *J. Afr. Earth Sci.* 61, 142–159. <https://doi.org/10.1016/j.jafrearsci.2011.06.003>.
- Fedo, C.M., Eriksson, K.A., Blenkinsop, T.G., 1995. Geologic history of the Archean Buhwa Greenstone Belt and surrounding granite-gneiss terrane,

- Zimbabwe, with implications for the evolution of the Limpopo Belt. *Can. J. Earth Sci.* 32, 1977–1990. <https://doi.org/10.1139/e95-151>.
- Fedo, C.M., Young, G.M., Nesbitt, H.W., Hanchar, J.M., 1997. Potassic and sodic metasomatism in the southern province of the Canadian shield: evidence from the Paleoproterozoic serpent formation Huronian supergroup, Canada. *Precambrian Res.* 84, 17–36. [https://doi.org/10.1016/S0301-9268\(96\)00058-7](https://doi.org/10.1016/S0301-9268(96)00058-7).
- Feybesse, J.L., Johan, V., Maurizot, P., Abessolo, A., 1987. Evolution tectonométamorphique libérienne et éburnéenne de la partie NW du craton zairois (SW Cameroun). In: Mathéis, G., Schandlmeier, H. (Eds.), *Current Research in African Earth Sciences*. Balkema, Rotterdam, pp. 9–12.
- Floyd, P.A., Leveridge, B.E., 1987. Tectonic environments of the Devonian Gramscatho basin, south Cornwall: framework mode and geochemical evidence from turbidite sandstones. *J. Geol. Soc.* 144, 531–542. <https://doi.org/10.1144/gsjgs.144.4.0531>.
- Gallala, W., Gaied, M.E., Montacer, M., 2009. Detrital mode, mineralogy and geochemistry of the Sidi Aïch Formation (Early Cretaceous) in central and southwestern Tunisia: implication for provenance, tectonic setting and paleoenvironment. *J. Afr. Earth Sci.* 53, 159–170. <https://doi.org/10.1016/j.jafrearsci.2009.01.002>.
- Garzanti, E., Vermeesch, P., Vezzoli, G., Audiò, S., Botti, E., Limonta, M., Dinis, P., Hahn, A., Baudet, D., De Grave, J., Kitambala, Y.N., 2019. Congo River sand and the equatorial quartz factory. *Earth Sci. Rev.* 197, 102918. <https://doi.org/10.1016/j.earscirev.2019.102918>.
- Garzanti, E., He, J., Barbarano, M., Resentini, A., Chao, L., Lu, Y., Shouye, Y., Hua, W., 2020. Provenance versus weathering control on sediment composition in tropical monsoonal climate (South China) - 2. Sand petrology and heavy minerals. *Chem. Geol.* 1–51. <https://doi.org/10.1016/j.chemgeo.2020.119860>.
- Garzanti, E., He, J., Barbarano, M., Resentini, A., Li, C., Yang, L., Wang, H., 2021. Provenance versus weathering control on sediment composition in tropical monsoonal climate (South China)-2. Sand petrology and heavy minerals. *Chem. Geol.* 564, 119997. <https://doi.org/10.1016/j.chemgeo.2020.119997>.
- Gazel, J., Guiraudie, C., 1965. *Carte géologique de reconnaissance à l'échelle 1/500 000, feuille Abong-Mbang Ouest, plus notice explicative*. Imprimerie nationale de Yaoundé, p. 28.
- Gu, X.X., Liu, J.M., Zheng, M.H., Tang, J.X., Qi, L., 2002. Provenance and Tectonic Setting of the Proterozoic Turbidites in Hunan, South China: Geochemical Evidence. *J. Sediment. Res.* 72, 393–407. <https://doi.org/10.1306/081601720393>.
- Harnois, L., 1988. The CIW index: a new chemical index of weathering. *Sediment. Geol.* 55, 319–322. [https://doi.org/10.1016/0037-0738\(88\)137-6](https://doi.org/10.1016/0037-0738(88)137-6).
- Hayashi, K.I., Fujisawa, H., Holland, H.D., Ohmoto, H., 1997. Geochemistry of 1.9 Ga sedimentary rocks from northeastern Labrador, Canada. *Geochim. Cosmochim. Acta* 61, 4115–4137. [https://doi.org/10.1016/S0016-7037\(97\)00214-7](https://doi.org/10.1016/S0016-7037(97)00214-7).
- Herron, M.M., 1988. Geochemical classification of terrigenous sands and shales from core or log data. *J. Sediment. Petrol.* 58, 820–829. <https://doi.org/10.1306/212F8E77-2B24-11D7-8648000102C1865D>.
- Jian, X., Zhang, W., Yang, S., Kao, S.J., 2020. Climate-dependent sediment composition and transport of mountainous rivers in tectonically stable, subtropical East Asia. *Geophys. Res. Lett.* 47, e2019GL086150. <https://doi.org/10.1029/2019GL086150>.
- Karam, R., 2019. Valorization de sédiments marins non calcinés dans un climat alcali-activé à base de laitier de Haut-Fourneau. Ecole centrale de Nantes. Doctoral dissertation.
- Kirkwood, C., Everett, P., Ferreira, A., Lister, B., 2016. Stream sediment geochemistry as a tool for enhancing geological understanding: An overview of new data from south west England. *J. Geochem. Explor.* 163, 28–40. <https://doi.org/10.1016/j.gexplo.2016.01.010>.
- Kontchipe, Y.S.N., Sopie, F.T., Ngueutchoua, G., Sonfack, A.N., Nkouathio, D.G., Tchatchueng, R., Nguemo, G.R.K., Njanko, T., 2021. Mineralogy and geochemistry study of the Nyong River sediments, SW Cameroon: Implications for provenance, weathering, and tectonic setting. *Arab. J. Geosci.* 14, 1–26. <https://doi.org/10.1007/s12517-021-07145-9>.
- Kwewouo Janpou, A., Ngueutchoua, G., Eko Bessa, A.Z., Armstrong-Altrin, J.S., Kankeu Kayou, U.R., Njike Njome, M.O.A.N., Njanko, T., Amabassa Bela, V., Kanouo Tiotsop, M.S., Tankou, J.G., 2022. Composition, provenance, and weathering of beach sands close to volcanic rocks from the northern Gulf of Guinea, SW Cameroon. *J. Afr. Earth Sci.* 188, 104473. <https://doi.org/10.1016/j.jafrearsci.2022.104473>.
- Lee, Y.I., 2009. Geochemistry of shales of the Upper Cretaceous Hayang Group, SE Korea: implications for provenance and source weathering at an active continental margin. *Sediment. Geol.* 215, 1–12. <https://doi.org/10.1016/j.sedgeo.2008.12.004>.
- Lerouge, C., Cocherie, A., Toteu, S.F., Penaye, J., Miñesi, J.-P., Tchameni, R., Nsifa, E.N., Fanning, C.M., Deloule, E., 2006. Shrimp U-Pb zircon age evidence for paleoproterozoic sedimentation and 2.05 Ga syntectonic plutonism in the Nyong group: consequences for the Eburnean-Transamazonian belt of NE Brasil and central Africa. *J. Afr. Earth Sci.* 44, 413–427. <https://doi.org/10.1016/j.jafrearsci.2005.11.010>.
- Letouzey, R., 1985. Notice de la carte phytogéographique du Cameroun au 1/500.000. Institut de Recherche Agricole de Yaoundé et Institut de Cartographie Internationale. Végétation, Toulouse, p. 240p.
- Liu, Z., Zhao, Y., Colin, C., Stattegger, K., Wiesner, M.G., Huh, C.-A., Zhang, Y., Li, X., Sompongchaiyakul, P., You, C.-F., Huang, C.-Y., Liu, J.T., Siriring, F.P., Le, K.P., Sathiamurthy, E., Hantoro, W.S., Liu, J., Tuo, S., Zhao, S., Zhou, S., He, Z.W.Y., Bunsomboonsakul, S., Li, Y., 2016. Source-to-sink transport processes of fluvial sediments in the South China Sea. *Earth Sci. Rev.* 153, 238–273. <https://doi.org/10.1016/j.earscirev.2015.08.005>.
- Madhavaraju, J., 2015. Geochemistry of late cretaceous sedimentary rocks of the Cauvery Basin, south India: constraints on paleoweathering, provenance, and end Cretaceous environments. *Chemostratigraphy* 185–214. <https://doi.org/10.1016/B978-0-12-419968-2.00008-x>.
- Madhavaraju, J., Lee, Y.I., 2010. Influence of Deccan volcanism in the sedimentary rocks of Late Maastrichtian-Danian age of Cauvery Basin, Southeastern India: constraints from geochemistry. *Curr. Sci.* 98, 528–537.
- Madhavaraju, J., Ramírez-Montoya, E., Monreal, R., González-León, C.M., Pi-Puig, T., Espinoza-Maldonado, I.G., Grijalva-Noriega, F.J., 2016. Paleoclimate, paleoweathering and paleoredox conditions of Lower Cretaceous shales from the Mural Limestone, Tuape section, northern Sonora, Mexico: constraints from clay mineralogy and geochemistry. *Rev. Mex. Ciencias Geol.* 33, 34–48.
- Mbabi Bitchong, A., Adatte, T., Ngon, G.F.N., Ngos, S., Bilong, P., 2021. Palynology, mineralogy and geochemistry of sediments in Tondé locality, northern part of Douala sub-basin, Cameroon, Central Africa: implication on paleoenvironment. *Geosci. J.* 25, 299–319. [https://doi.org/10.1007/s12303\\_020\\_0021-z](https://doi.org/10.1007/s12303_020_0021-z).
- Mbale Ngama, E., Sababa, E., Bayiga, E.C., Eko Bessa, A.Z., Ndjigui, P.D., Bilong, P., 2019. Mineralogical and geochemical characterization of the unconsolidated sands from the Mefou River terrace, Yaoundé area, Southern Cameroon. *J. Afr. Earth Sci.* 159, 103570. <https://doi.org/10.1016/j.jafrearsci.2019.103570>.
- Nagarajan, R., Armstrong-Altrin, J.S., Nagendra, R., Madhavaraju, J., Moutte, J., 2007. Petrography and geochemistry of terrigenous sedimentary rocks in the Neoproterozoic Rabanpalli formation, Bhima Basin, northern Karnataka, Southern India: implications for paleoweathering condition, provenance, and source rocks composition. *J. Geol. Soc. India* 70, 297–312.
- Nakao, A., Sugihara, S., Maejima, Y., Tsukada, H., Funakawa, S., 2017. Ferralsols in the Cameroon plateaus, with a focus on the mineralogical control on their cation exchange capacities. *Geoderma* 285, 206–216. <https://doi.org/10.1016/j.geoderma.2016.10.003>.
- Nanga Bineli, M.T., Onana, V.L., Noa Tang, S.D., Bikoy, Y.R., Ekodeck, G.E., 2020. Mineralogy and geochemistry of sands of the lower course of the Sanaga River, Cameroon: implications for weathering, provenance, and tectonic setting. *Acta Geochim.* 40, 348–365. <https://doi.org/10.1007/s11631-020-00437-z>.
- Ndjigui, P.-D., Ebah Abeng, S.A., Ekomane, E., Nzeukou, N.A., Ngo Mandeng, F.S., Lindjeck, M.M., 2015. Mineralogy and geochemistry of pseudogley soils and recent alluvial clastic sediments in the Ngog-Lituba

- region, Southern Cameroon: an implication to their genesis. *J. Afr. Earth Sci.* 108, 1–14. <https://doi.org/10.1016/j.jafrearsci.2015.03.023>.
- Ndjigui, P.-D., Onana, V.L., Sababa, E., Bayiga, E.C., 2018. Mineralogy and geochemistry of the Lokoundje alluvial clays from the Kribi deposits, Cameroonian Atlantic coast: implications for their origin and depositional environment. *J. Afr. Earth Sci.* 143, 102–117. <https://doi.org/10.1016/j.jafrearsci.2018.03.023>.
- Ndjigui, P.-D., Bayiga, E.C., Onana, V.L., Djenabou-Fadil, S., Ngonon, G.S.A., 2019. Mineralogy and geochemistry of recent alluvial sediments from the Ngaye River water shed, northern Cameroon: implications for the surface processes and Au-PGE distribution. *J. Afr. Earth Sci.* 150, 136–157. <https://doi.org/10.1016/j.jafrearsci.2018.10.012>.
- Nesbitt, H., Young, G.M., 1982. Early Proterozoic climates and plate motions inferred from major element chemistry of lutites. *Nature* 299, 715–717. <https://doi.org/10.1038/299715a0>.
- Ngnotué, T., Nzenti, J.P., Barbey, P., Tchoua, F.M., 2000. The Ntui-Betamba highgrade gneisses: a Northward extension of the Pan-African Yaoundé gneisses in Cameroon. *J. Afr. Earth Sci.* 31, 369–381. [https://doi.org/10.1016/S0899-5362\(00\)00094-4](https://doi.org/10.1016/S0899-5362(00)00094-4).
- Ngnotué, T., Ganno, S., Nzenti, J.P., Schulz, B., Tchaptchet Tchato, D., Suh Cheo, E., 2012. Geochemistry and geochronology of Peraluminous High-K granitic leucosomes of Yaoundé series (Cameroon): evidence for a unique Pan-African magmatism and melting event in North Equatorial Fold Belt. *Int. J. Geosci.* 3, 525–548. <https://doi.org/10.4236/ijg.2012.33055>.
- Ngon Ngon, G.F., Etame, J., Ntamak-Nida, M.J., Mbesse, O.C., Mbai, J.S., Bayiga, E.C., Gerard, M., 2016. Geochmical and paleoenvironmental characteristics of Missole I iron duricrusts of the Douala sub-basin (Western Cameroon). *Compt. Rendus Geosci.* 348, 127–137.
- Ngueutchoua, G., Ngantchu, L.D., Youbi, M., Ngos III, S., Beyala, V.K.K., Yifomju, K.P., Tchamgoué, J.C., 2017. Geochemistry of Cretaceous mudrocks and sandstones from Douala sub-basin, Kumba area, South West Cameroon: constraints on provenance, source rock weathering, paleo-oxidation conditions and tectonic environment. *Int. J. Geosci.* 8, 393–424. <https://doi.org/10.4236/ijg.2017.84021>.
- Ngueutchoua, G., Eko Bessa, A.Z., Eyong, T.J., Zandjio, D.D., Baba, B.H., Tchami, N.L., 2019a. Geochemistry of Cretaceous mudrocks and sandstones from Douala sub-basin, SW Cameroon: implications for weathering intensity, provenance, paleoclimate, redox condition, and tectonic setting. *J. Afr. Earth Sci.* 152, 215–236. <https://doi.org/10.1016/j.jafrearsci.2019.02.021>.
- Ngueutchoua, G., Eyong, J.T., Eko Bessa, A.Z., Agheenwi, Z.B.A., Maschouer, A.E., Kemteu, C.S., Nguemo, G.R.K., 2019b. Provenance and depositional history of Mesozoic sediments from the Mamfe basin and Douala sub-basin (SW Cameroon) unraveled by geochemical analysis. *J. Afr. Earth Sci.* 158, 103–550. <https://doi.org/10.1016/j.jafrearsci.2019.103550>.
- Noa Tang, S.D., Ntsama Atangana, J., Onana, V.L., 2020. Mineralogy and geochemistry of alluvial sediments from the Kadéy plain, eastern Cameroon: Implications for provenance, weathering, and tectonic setting. *J. Afr. Earth Sci.* 1–17. <https://doi.org/10.1016/j.jafrearsci.2020.103763>.
- Nomo, N.E., Tchameni, R., Vanderhaeghe, O., Sun, F., Barbey, P., Tekoum, F.T.P.M., Eglinger, A., Saha, F.N.A., 2017. Structure and LA-ICP-MS zircon U-Pb dating of syn-tectonic plutons emplaced in the Pan-African Banyo-Tchollire shear zone (Central north Cameroon). *J. Afr. Earth Sci.* 133, 251–271. <https://doi.org/10.1016/j.jafrearsci.2017.04.002>.
- Nzenti, J.P., Ngako, V., Kambou, R., Penaye, J., Bassahak, J., et Njel, U.O., 1992. Structures régionales de la chaîne panafricaine du Nord Cameroun. *C. R. Acad. Sci.* 315, 209–215.
- Nzenti, J.P., Abaga, B., Suh, C.E., Nzolang, C., 2011. Petrogenesis of per-aluminous magmas from the Akum-Bamenda Massif, Pan-African Fold Belt, Cameroon. *Int. Geol. Rev.* 53, 1121–1149. <https://doi.org/10.1080/00206810903442402>.
- Nzolang, C., Kagami, H., Nzenti, J.P., Holtz, F., 2003. Geochemistry and preliminary Sr-Nd isotopic data on the Neoproterozoic granitoids from the Bantoun area, west Cameroon: evidence for a derivation from a paleoproterozoic to Archean crust. *Polar Geosci.* 16, 196–226. <https://doi.org/10.15094/00003129>.
- N'Nanga, A., Simon III, N., Gabriel, N., 2019. The Late Pleistocene Holocene paleoclimate reconstruction in the Adamawa plateau (Central Cameroon) inferred from the geochemistry and mineralogy of the Lake Fonjak sediments. *J. Afr. Earth Sci.* 150, 23–36. <https://doi.org/10.1016/j.jafrearsci.2018.09.024>.
- Owona, S., Schulz, B., Ratschbacher, L., Mvondo Ondo, J., Ekodeck, G.E., Tchoua, M.F., Affaton, P., 2011. Pan-African metamorphic evolution in the Southern Yaoundé Group (Oubanguide Complex, Cameroon) as revealed by EMP-Monazite dating and thermobarometry and garnet metapelites. *J. Afr. Earth Sci.* 59, 125–139. <https://doi.org/10.1016/j.jafrearsci.2010.09.003>.
- Owona, S., Ratschbacher, L., Nsangou, N.M., Gulzar, A.M., Mvondo, O.J., Ekodeck, G.E., 2021. How diverse is the source? Age, provenance, reworking, and overprint of Precambrian meta-sedimentary rocks of West Gondwana, Cameroon, from zircon U-Pb geochronology. *Precambrian Res.* 359, 106220. <https://doi.org/10.1016/j.precamres.2021.106220>.
- Penaye, J., Nzenti, J.P., Toteu, S.F., Van Scmus, W.R., et Nzenti, J.P., 1993. U-Pb and SmNd preliminary geochronologic data on the Yaoundé series, Cameroon: re-interpretation of the granulitic rocks as the suture of a collision in the "centrafrican" belt. *C. R. Acad. Sci.* 317, 789–794.
- Ramamoorthy, A., Nazir, S.R.N., 2020. Provenance, tectonic settings and weathering of Gondwana sediments, Lingaraj area, Talchir, Odisha, India - insights from petrography, heavy minerals, x ray diffraction and geochemistry. *Sci. Technol. Dev.* 9, 291–336.
- Ramírez-Montoya, E., Madhavaraju, J., González-León, C.M., Armstrong-Altrin, J.S., Monreal, R., 2022. Detrital Zircon Geochemistry in the Morita Formation, Northern Sonora, Mexico: Implications for Origin and Source Rock Type. In: Armstrong-Altrin, J.A., Pandarinath, K., Verma, S. (Eds.), *Geochemical Treasures and Petrogenetic Processes*, pp. 315–350. [https://doi.org/10.1007/978-981-19-4782-7\\_12](https://doi.org/10.1007/978-981-19-4782-7_12).
- Ramos-Vázquez, M.A., Armstrong-Altrin, J.S., 2020. Provenance and palaeoenvironmental significance of microtextures in quartz and zircon grains from the Paseo del Mar and Bosque beaches, Gulf of Mexico. *J. Earth Syst. Sci.* 129, 1–16. <https://doi.org/10.1007/s12040-020-01491-0>.
- Ramos-Vázquez, M.A., Armstrong-Altrin, J.S., Madhavaraju, J., Gracia, A., Salas-de-León, D.A., 2022. Mineralogy and geochemistry of marine sediments in the Northeastern Gulf of Mexico. In: Armstrong-Altrin, J.A., Pandarinath, K., Verma, S. (Eds.), *Geochemical Treasures and Petrogenetic Processes*, pp. 153–183. [https://doi.org/10.1007/978-981-19-4782-7\\_7](https://doi.org/10.1007/978-981-19-4782-7_7).
- Ramos-Vazquez, M.A., Armstrong-Altrin, J.S., 2019. Sediment chemistry and detrital zircon record in the Bosque and Paseo del Mar coastal areas from the southwestern Gulf of Mexico. *Mar. Petrol. Geol.* 110, 650–675. <https://doi.org/10.1016/j.marpetgeo.2019.07.032>.
- Rao, W., Tan, H., Jiang, S., Chen, J., 2011. Trace element and REE geochemistry of fine and coarse-grained sands in the Ordos deserts and links with sediments in surrounding areas. *Geochemistry* 71, 155–170. <https://doi.org/10.1016/j.chemer.2011.02.003>.
- Roser, B.P., Korsch, R.J., 1988. Provenance signatures of sandstone-mudstone suites determined using discriminant function analysis of major-element data. *Chem. Geol.* 67, 119–139. [https://doi.org/10.1016/0009-2541\(88\)90010-1](https://doi.org/10.1016/0009-2541(88)90010-1).
- Roy, P.D., Caballero, M., Lozano, R., Smykatz-Kloss, W., 2008. Geochemistry of Late Quaternary sediments from Tecocomulco Lake, central Mexico: implication to chemical weathering and provenance. *Chem. Erde* 68, 383–393. <https://doi.org/10.1016/j.chemer.2008.04.001>.
- Schneider, G., 2001. Boues de curage des cours d'eau. *Courr. Environ. INRA* 43, 146–147.
- Shang, C.K., Satir, M., Siebel, W., Nsifa, E.N., Taubald, H., Liégeois, J.-P., Tchoua, F.M., 2004. TTG magmatism in the Congo craton; a view from major and trace element geochemistry, Rb-Sr and Sm-Nd systematics: case of the Sangmelima region, Ntem complex, southern Cameroon. *J. Afr. Earth Sci.* 40, 61–79. <https://doi.org/10.1016/j.jafrearsci.2004.07.005>.
- Shang, C.K., Satir, M., Nsifa, E.N., Liégeois, J.P., Siebel, W., Taubald, H., 2007. Archaean high-k granitoids produced by remelting of earlier Tonalite-Trondhjemite-Granodiorite (TTG) in the Sangmelima region of the

- Ntem complex of the Congo craton, southern Cameroon. *Int. J. Earth Sci.* 96, 817–841. <https://doi.org/10.1007/s00531-006-0141-3>.
- Shang, C.K., Liégeois, J.P., Satir, M., Frisch, W., Nsifa, E.N., 2010. Late Archaean high-K granite geochronology of the northern metacratonic margin of the Archaean Congo craton, Southern Cameroon: Evidence for Pb-loss due to non-metamorphic causes. *Gondwana Res.* 18, 337–355. <https://doi.org/10.1016/j.gr.2010.02.008>.
- Silva, M.M.V.V., Pinto, M.M.S.C., Carvalho, P.C.S., 2016. Major, trace and REE geochemistry of recent sediments from lower Catumbela River (Angola). *J. Afr. Earth Sci.* 115, 203–217. <https://doi.org/10.1016/j.jafrearsci.2015.12.014>.
- Sonfack, A.N., Ngueutchoua, G., Kontchipe, Y.S.N., Sopie, F.T., Nkouathio, D.G., Wouatong, A.S.L., Njanko, T., 2021. Mineralogical and geochemical signatures of surface stream sediments from Dibamba River basin, SW Cameroon: Implications for provenance, weathering, and tectonic setting. *J. Afr. Earth Sci.* 181, 104251. <https://doi.org/10.1016/j.jafrearsci.2021.104251>.
- Tchakounté, J.N., Gentry, F.C., Kamwa, A.N., Victor, M., Ondo, J.M., Nkoumbou, C., 2021. Petrology and geochemistry of the Pan-African High-K calc-alkaline to shoshonitic-adakitic Bapé plutonic suites (Adamawa-Yade block, Cameroon): evidence of a hot oceanic crust subduction. *Int. J. Earth Sci.* <https://doi.org/10.1007/s00531-021-02060-6>.
- Tchameni, R., Mezger, K., Nsifa, N.E., Pouclet, A., 2000. Neoarchean crustal evolution in the Congo craton: evidence from the K-rich granitoids of the Ntem Complex, Southern Cameroon. *J. Afr. Earth Sci.* 30, 133–147. [https://doi.org/10.1016/S0899-5362\(00\)00012-9](https://doi.org/10.1016/S0899-5362(00)00012-9).
- Tchouatcha, M.S., Kouske, A.P., Said Deaf, A., Mioumnde, A.P., 2021. Geochemical, mineralogical and sedimentological analyses of reworked sediments (new) in the syn-to post-rift Middle Cretaceous-Quaternary detrital deposits from western Atlantic margin of Cameroon: evidence from sedimentation-erosion alternation in the context of passive margin evolution. *Acta Geochem.* <https://doi.org/10.1007/s11631-021-00455-5>.
- Temga, J.P., Azinwi, T.P., Basga, D.S., Zo'o Zame, P., Gouban, H., Abossolo, M., Nguetnkam, J.P., Bitom, D.L., 2019. Characteristics, classification and genesis of vertisols under seasonally contrasted climate in the Lake Chad basin, Central Africa. *J. Afr. Earth Sci.* 150, 176–193. <https://doi.org/10.1016/j.jafrearsci.2018.11.003>.
- Temga, J.P., Sababa, E., Mamdem, L.E., Ngo Bijeck, M.L., Azinwi, P.T., Tehna, N., Zame, P.Z., Onana, V.L., Nguetnkam, J.P., Bitom, L.D., Ndjigui, P.-D., 2021. Rare earth elements in tropical soils, Cameroon soils (Central Africa). *Geoderma Regional* 25, e00369. <https://doi.org/10.1016/j.geodrs.2021.e00369>.
- Tiju, I.V., Prakash, T.N., Nagendra, R., Nagarajan, R., 2018. Sediment geochemistry of coastal environments, southern Kerala, India: implication for provenance. *Arab. J. Geosci.* 11 (61). <https://doi.org/10.1007/s12517-018-3406-9>.
- Toteu, S.F., Penaye, J., Djomani Poudjom, Y., 2004. Geodynamic evolution of the PanAfrican belt in Central Africa with special reference to Cameroon. *Can. J. Earth Sci.* 41, 73–85. <https://doi.org/10.1139/e03-079>.
- Tsozue, D., Ndjigui, P.-D., 2017. Geochemical features of the weathered materials developed on gabbro in the semi-arid zone, Northern Cameroon. *Geosciences* 7, 16. <https://doi.org/10.3390/geosciences7020016>.
- Verma, S.P., Armstrong-Altrin, J.S., 2016. Geochemical discrimination of siliciclastic sediments from active and passive margin settings. *Sediment. Geol.* 332, 1–12. <https://doi.org/10.1016/j.sedgeo.2015.11.011>.
- Yu, L., Zou, S., Cai, J., Xu, D., Zou, F., Wang, Z., Wu, C., Liu, M., 2016. Geochemical and Nd isotopic constraints on provenance and depositional setting of the Shi-Huiding Formation in the Shilu Fe-Co-Cu ore district, Hainan Province, south China. *J. Asian Earth Sci.* 119, 100–117. <https://doi.org/10.1016/j.jseas.2016.01.015>.
- Zaid, S.M., 2012. Provenance, diagenesis, tectonic setting and geochemistry of rudies sandstone (lower Miocene), warda field, Gulf of Suez, Egypt. *J. Afr. Earth Sci.* 66, 56–71. <https://doi.org/10.1016/j.jafrearsci.2012.03.008>.